ENVIRONMENTAL RESEARCH
LETTERS

PURPOSE-LED PUBLISHING™

Part of the
ENVIRONMENTAL RESEARCH
SERIES

LETTER • OPEN ACCESS

Unequal economic consequences of coastal hazards: hurricane impacts on North Carolina

To cite this article: Dahui Liu *et al* 2024 *Environ. Res. Lett.* **19** 104003

IOP Publishing Environ. Res. Lett. 19 (2024) 104003 https://doi.org/10.1088/1748-9326/ad6d81

ENVIRONMENTAL RESEARCH
LETTERS

OPEN ACCESS

RECEIVED
19 December 2023

REVISED
6 August 2024

ACCEPTED FOR PUBLICATION
9 August 2024

PUBLISHED
23 August 2024

LETTER

Unequal economic consequences of coastal hazards: hurricane impacts on North Carolina

Dahui Liu[1,*], **Junkan Li**[2], **Ian Sue Wing**[3], **Brian Blanton**[4], **Jamie Kruse**[5], **Linda Nozick**[2] and **Meghan Millea**[5]

[1] Glorious Sun School of Business and Management, Donghua University, Shanghai 200051, People's Republic of China
[2] School of Civil and Environmental Engineering, Cornell University, Ithaca, NY, United States of America
[3] Department of Earth & Environment, Boston University, Boston, MA, United States of America
[4] Renaissance Computing Institute, UNC Chapel Hill, Chapel Hill, NC, United States of America
[5] Department of Economics, East Carolina University, Greenville, NC, United States of America
[*] Author to whom any correspondence should be addressed.

E-mail: dlkevin@dhu.edu.cn

Keywords: natual hazards, economic consequences, capital and labor losses, social vulnerability, asset values

Abstract

The eastern North Carolina Coastal Area Management Act region is one of the most hurricane-prone areas of the United States. Hurricanes incur substantial damage and economic losses because structures located near the coast tend to be high value as well as particularly exposed. To bolster disaster mitigation and community resilience, it is crucial to understand how hurricane hazards drive social and economic impacts. We integrate detailed hazard simulations, property data, and labor compensation estimates to comprehensively analyze hurricanes' economic impacts. This study investigates the spatial distribution of probabilistic hurricane hazards, and concomitant property losses and labor impacts, pinpointing particularly hard hit areas. Relationships between capital and labor losses, social vulnerability, and asset values reveal the latter as the primary determinant of overall economic consequences.

1. Introduction

Hurricanes are the most costly type of natural disaster in the United States (Smith and Katz 2013, NCEI 2023), with property damage being a major driver of economic losses. Coastal and peri-coastal development has led to structures being located in areas that are at risk of tropical storm-force winds and surge flooding, increasing the exposure of residential and nonresidential assets. Along the Atlantic and Gulf coasts, built up areas experiencing >6 m s^{-1} average maximum wind gust speed exposures have nearly doubled since 1980—with low- and medium-density development accounting for the bulk of such areas in high-risk locations such as eastern North Carolina (NC) (Iglesias *et al* 2021). Under the 2022 Community Disaster Resilience Zones Act, the Federal Emergency Management Agency (FEMA) must 'identify census tracts which are most at risk from the effects of natural hazards and climate change.' Of the thirteen NC tracts thus designated, all but one are in Coastal Area Management Act (CAMA) counties.

Prior research has sought to normalize trends in recorded hurricane losses (typically, insurance claims—e.g. Smith and Matthews 2015, Bakkensen *et al* 2018) as a way of disentangling the contributions of hazard characteristics (Zhai and Jiang 2014) and their potential climate-change driven intensification (Pielke 2021), development-driven increases in exposure, building-code/-quality driven declines in the susceptibility of assets to damage (e.g. Done *et al* 2018), as well as the interactions among these drivers (Nair *et al* 2020). A particular concern is the manner in which losses scale with income, and the implications for inequality in the burden of hurricane risk. Geiger *et al* (2016) find that U.S. hurricane losses increase sub-linearly with exposed population and supra-linearly with per capita income, but their inference relies on population-downscaled state GDP as a proxy for exposure, and its robustness is contested (Geiger *et al* 2016, Rybski *et al* 2017).

Underlying such aggregate trends are socioeconomic processes that act in opposing directions. Properties located close to the coast are proximate to amenities (e.g. viewsheds, water recreation accessibility) that command a price premium, but such properties are also more exposed to the disamenity of coastal hazards (e.g. storm surge, hurricane force winds without the shielding effects of terrain) and associated price discounts. Holding constant hazard exposures as well as property vulnerability and damage, areas with higher-income, less socially vulnerable populations who can afford expensive housing will tend to incur larger total losses simply because exposed assets are worth more. Conversely, marginalized populations (who are disproportionately adversely impacted by major hurricanes—Benevolenza and DeRigne 2019) tend to reside in relatively low-cost, low-value areas and housing contexts. In a competitive economic equilibrium, the former discounts would provide actuarially fair compensation for the disutility of elevated hazard exposure as well as damage susceptibility, leading to sorting of low-income, more socially vulnerable residents into harm's way. This outcome is consistent with findings of a high degree of overlap between areas of high flood exposure and high social vulnerability, in Louisiana (Shao *et al* 2020) and across the broader southeastern US (Tate *et al* 2021).

These two phenomena highlight the question that motivates the present study: do hurricane losses respond more to asset values—and thus tend to decline with social vulnerability, or hazard exposure and damage susceptibility—and tend to increase with social vulnerability? Evidence is circumstantial and inconclusive. Examining the impact of hurricane Katrina on Mississippi's Gulf coast, Burton (2010) found extensive overlap among areas with the largest residential building damage (but not monetary losses) and high social vulnerability, with indicators of the latter having statistically significant explanatory power in census tracts where damage was extensive or catastrophic. The empirical economic literature has uncovered copious evidence of hazard risk signals in property markets. Sale prices of homes are significantly discounted due to exposure to future sea level rise (Bernstein *et al* 2021), inundation from hurricane Sandy—even for properties that did not sustain direct damage (Ortega and Taspinar 2018), and a proxy for pluvial risk constructed by interacting storm runoff percentiles with stationary flood depth exposures on different return periods (Pollack *et al* 2023). However, hedonic analyses that focus on mean estimates shed little light on whether hazard discounts vary with household incomes, property values or other correlates of social vulnerability in ways distinct from exposures.

Perhaps the closest to a direct answer is Nair *et al* (2020), who find that the balance between the risk discount and the amenity premium is heterogeneous over broad geographic scales. They attribute losses in peninsular Florida to socioeconomic exposure and vulnerability, but losses in the central Gulf Coast to the multiplicative interaction between climate hazards and socioeconomic exposure/vulnerability. But at finer spatial scales, Pollack *et al's* (2023) finding of no statistically significant discount for properties close to the shoreline suggests that the amenity premium dominates along the coast, where prices are often substantially higher compared to similar properties inland. Similarly, the degree of housing market overvaluation due to undercapitalization of flood hazards is particularly large along the Atlantic and Gulf coasts, both in dollar values and as a percentage of observed property values Gourevitch *et al* (2023). The suggestion is that asset values may be the dominant driver of coastal hazard losses.

The paper's approach to reconciling these disparate findings differs from the top–down empirical analyses of the determinants of insured losses or property prices cited above. We make three contributions. First, we extend Pollack *et al's* (2022) bottom-up approach, computing losses by combining hazard outputs from simulations of multiple synthetic hurricane events with data on the locations, vulnerabilities to wind speeds and flood depths, and values, of ∼1.6 million structures across the 44-county eastern NC coastal region. Second, we develop and apply a novel quasi-empirical model to estimate the short-run consequences of property damage for labor compensation. The latter declines in response to tropical cyclone shocks—especially among low-income individuals (Wu *et al* 2019)—as residents and firms reallocate time away from labor and production of output to remediating damage to residences and business establishments, respectively: opportunity costs that increase with damage severity (Groen *et al* 2020). Third, we aggregate structure and labor losses to the scale of census tracts and elucidate their relationship with social vulnerability scores, disentangling the relative importance of the exposure and asset effects described above. Our main finding is that the intensity of both capital losses and forgone labor earnings are negatively correlated with social vulnerability, a result that can be traced to the inverse relationship between vulnerability and the benchmark value of exposed assets.

2. Data and methods

2.1. Data

2.1.1. Hurricanes and hazard modeling

NC is one of the world's most hurricane-prone areas, experiencing more than 60 storm events over the past century (Landsea and Franklin 2013). Hurricanes exert substantial impacts on its coastal environment due to both strong wind gusts and storm surge driven toward and onto land by onshore winds. Given hurricanes' rarity (category 2 or greater hurricanes impact the NC coast with an annual occurrence probability of about 0.3—Landsea and Franklin 2013), the historical record is generally too short to adequately represent the true spatial and temporal extent of the hazard. Risk assessment requires the hurricane population to be 'inflated' to capture the full range of probable events. Two approaches are typically used. The first is the joint probability method, which generates combinations of attributes such as central pressure, radius of maximum winds, translation speed by sampling from the observed distributions of these parameters while accounting for known correlations among them (Vickery and Blanton 2008, Toro *et al* 2010). The resulting parameter sets are then distributed over a set of hypothetical but realistic track shapes. The second is a stochastic empirical track model (ETM) that generates a large set of events by sampling cyclone parameter distributions, genesis and lysis rates, and genesis locations, and computing storm trajectories by integrating displacement distributions, terminating a storm when specific criteria are met (e.g. lysis characteristics, distance onto continental land area, insufficient environmental conditions).

Here we use stochastic hurricane tracks from Vickery and Blanton (2008), generated using the ETM (Vickery *et al* 2000) to compute a synthetic and long-term storm event set that impacts the NC coast. More specifically, the ETM dataset was originally developed as part of a FEMA-funded coastal hazard analysis for the NC coast (Vickery and Blanton 2008, Blanton *et al* 2012). It included observed cyclone parameters through the year 2007 to generate a 10 000 year storm population for the entire North Atlantic basin. Each storm track in the ETM dataset is described by longitude/latitude position, and cyclone parameters such as central pressure and radius to maximum winds. As described in Apivatanagul *et al* (2011), the large candidate set of storms was reduced to an ensemble of 97 events that approximate the quantiles of distribution of the storm surge and wind speed hazards. Importantly, this method enables the assignment of an annual probability to each storm, facilitating computation of the moments of hazard exposures and losses. The 97 tracks are shown in figure A1, panel (A), colored by the central pressure, with the thick track indicating the most intense storm. (Storm parameter distributions are shown in figure A1, panels (B) and (C))

For each hurricane event, coastal storm surge and wind speeds are computed using the ADCIRC model (Luettich and Westerink 1992, Westerink *et al* 2008), a linear, triangular finite-element simulation that solves a form of the shallow water wave equations. ADCIRC has been applied extensively to investigate regional and local tidal phenomena and coupled storm surge and wave hindcasts (Blanton *et al* 2004, Atkinson *et al* 2008, Dietrich *et al* 2010), and develop comprehensive hazard datasets for use in FEMA's coastal flood insurance studies for the US Atlantic and Gulf coasts (e.g. Niedoroda *et al* 2010, Blanton *et al* 2012, Hanson *et al* 2013).

Apivatanagul *et al* (2011) ran ADCIRC in its two-dimensional, depth-integrated form on a ∼500 m grid in the NC coastal area. Land elevations and water bottom depths, frictional characteristics, land roughness lengths, and canopy cover are specified at each triangle centroid, or node, using available digital elevation models and land cover databases (e.g. the USGS National Elevation Model (Gesch *et al* 2002) and the National Land Cover Database (Homer *et al* 2012)). The ADCIRC model configuration did not include tides or wind waves. Cyclone wind and pressure fields were computed using ADCIRC's internal vortex model, using storm parameters as defined in the 97-event ensemble. Specific parameter settings and configuration details were set the same as used for the FEMA study for coastal NC, detailed in Blanton *et al* (2012). Each simulation generated full time histories of the water levels and winds at each node (figure A2, panel (A)), from which maximum inundation (maximum water level—topographic elevation) and wind speeds were calculated and used as inputs into loss modeling. (Surge and wind speeds for the strongest storm are shown in figure A2, panel (B))

2.1.2. Assets

The catalog of potentially exposed assets comes from the National Structure Inventory (NSI—USACE 2022). The NSI records the geolocation, value, occupancy characteristics, and structural and economic attributes of individual buildings. Our study area encompasses approximately 1.6 million structures, two thirds of which are single-family homes. We use the structures' and ADCIRC nodes' geocodes to impute property-level maximum surge and wind hazard exposures for each storm (figure 1—expected values in panels (A) and (C), worst case values in panels (B) and (D)).

2.1.3. Hazus damage functions

The relationships that link individual buildings' flood and wind hazard exposures to the damage, loss of function and reduction in economic value they sustain, are taken from the Hazus (Vickery *et al* 2006, FEMA 2022a, 2022b). Following the approach used by Klima *et al* (2012), we extract hazard-damage relationships differentiated by building characteristics (e.g. roof and wall material, basement presence) and sector (28 detailed 'occupancy classes'), yielding damage functions for a reduced set of 39 structural archetypes that spans the universe of buildings in our

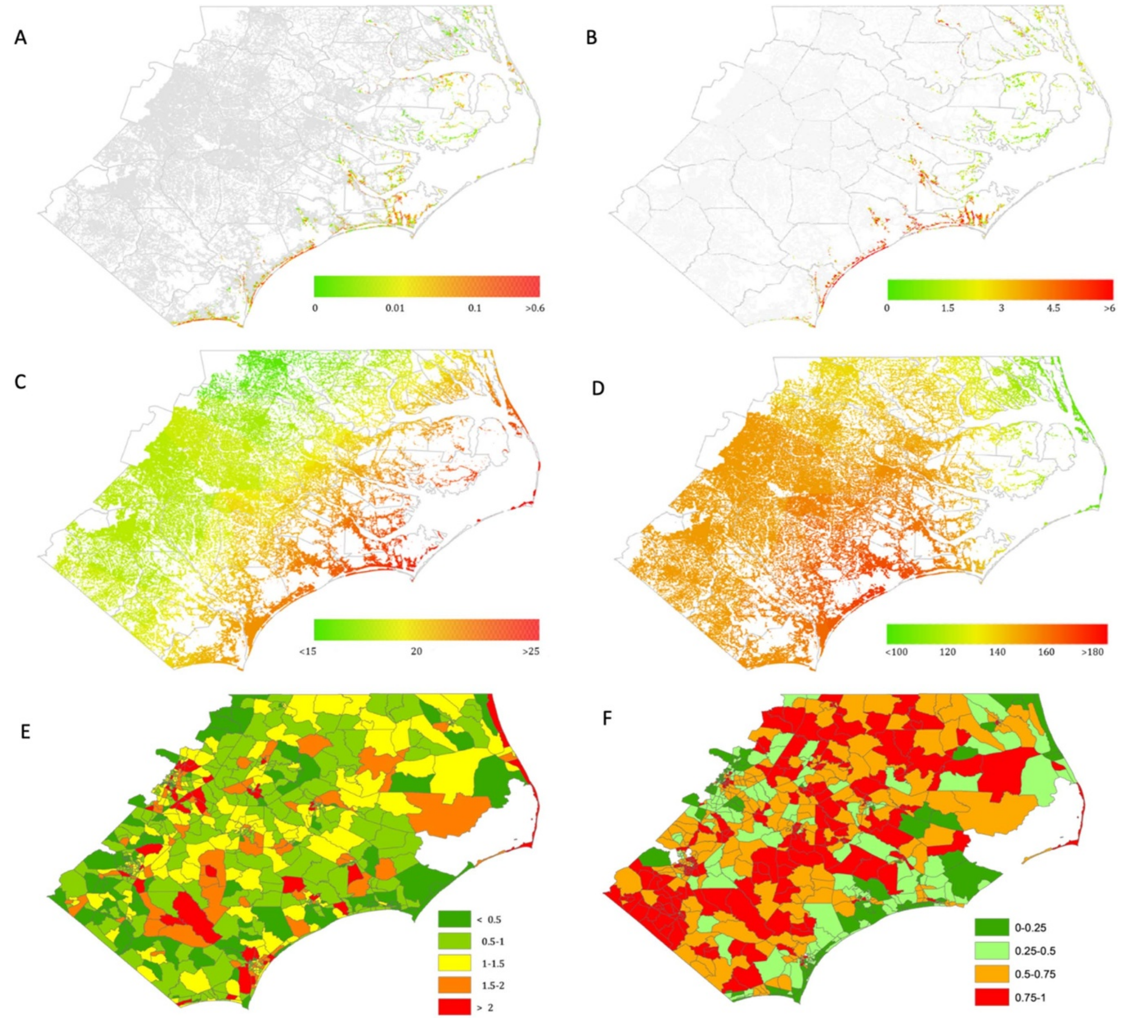

Figure 1. Hurricane hazards, property value and social vulnerability. (A), (B) Property-level expected and worst-case maximum storm surge depth (ft). (C), (D) Property-level expected and worst-case maximum wind speed (mph). (E), (F) Census tract value of buildings/contents (Bn $), and 2020 social vulnerability index.

NSI dataset (table A1, figures A3 and A4). Each individual building is then matched to an archetype based on its characteristics, enabling identical wind exposures to generate substantially different amounts of damage, depending on the building.

2.1.4. Employment and wages

To capture the potential impacts of property damage on jobs and labor compensation, we build on Belasen and Polachek (2008) and Metzler *et al* (2021), using the Longitudinal Employer Household Dynamics Origin-Destination Employment Statistics (LODES) dataset (US Census Bureau 2023). LODES tabulates annual commuting flows between census blocks, working population and number of jobs at each residence origin and workplace destination from 2002. LODES does not provide wage data directly, but apportions origin-destination flows into three broad wage intervals. For each class, we use American Community Survey annual microdata (Ruggles *et al* 2024) to calculate the average wage for workers in each wage interval in workplace tracts corresponding to census Public Use Microsample Areas (PUMAs—combinations of contiguous census tracts, the highest geographic resolution at which wages are available). The average wage calculated for each combination of PUMA and wage class is assigned to all workers within the same class in all workplace census tracts in that PUMA, and then calculate the average tract-level wages as the weighted average of the three wage classes, with tracts' shares of workers in each class as weights (see appendix)

2.1.5. Social vulnerability

To investigate inequality in the incidence of hurricane losses, we use the US Centers for Disease Control Agency for Toxic Substances and Disease Registry (CDC/ATSDR) social vulnerability index (SVI) for the year 2020 at the census tract level (Flanagan *et al* 2018). The index is an aggregate of 16 primary variables tabulated by the US Census, grouped into four themes (socioeconomic status, household characteristics, racial/ethnic minority status, housing type and transportation)[6].

2.2. Loss modeling

2.2.1. Capital losses

Our high-resolution asset data allow us to model capital losses at the scale of individual properties. Extending Pollack *et al* (2022), the indexes i = individual properties, g = matched hazard layer grid cells, O = occupancy classes, h = hazard types, j = economic sectors, and s = storm events. We also let the variables D^h denote property- and hazard-specific damage functions, v denote a property's value and x^h denote its hazard exposure. Property-level capital loss (KL) is then computed as

$$KL_{i,s} = \max_h \left\{ D^h_{o(i)} \left[x^h_{g(i),s} \right] \right\} \cdot v_i. \quad (1)$$

We sum these losses and the value of exposed property over areal units (indexed by a—i.e. census blocks, tracts and counties), and take the ratio to compute the sector-, area-, and storm-specific capital damage intensity:

$$\kappa_{j,a,s} = \sum_{o(i)\in j, i\in a} KL_{i,s} \Big/ \sum_{o(i)\in j, i\in a} v_i\,. \quad (2)$$

Using π_s to denote each storm's probability, the expected aggregate fractional loss is

$$\mathbb{E}[\kappa_a] = \sum_{o(i), i\in a} \sum_s \pi_s KL_{i,s} \Big/ \sum_{o(i), i\in a} v_i. \quad (3)$$

The critical implication that aggregates losses (e.g., at the census tract level) depend as much on the demography of exposed assets (distributions of damage susceptibility, D, value, v, and their correlation over space) as the details of the hazard field.

2.2.2. Labor losses

Labor losses are fundamentally driven by capital stock destruction. Damage to structures lowers local production capacity, generating excess demand for capital goods for reconstruction. In the aftermath of hurricanes there may be significant shortages of both labor and commodities that bid up wages and prices. We develop a simple model of the short-run equilibrium of the economy post-disaster to demonstrate the relevant mechanisms. Abstracting from the confounding effects of migration, our welfare indicator is the change in the per capita real earnings of a population of constant size. Using w and r to index census tracts of work and residence, letting N_r and E_r denote the baseline pre-storm event population and per capita real earnings of households residing in census tract r, labor losses can be expressed as:

$$LL_r(s) = \left(E_r^{\text{Hurricane}}(s) - E_r^{\text{Baseline}}\right) \cdot N_r \quad (4)$$

where, given residence-workplace commuting flows, F, workplace wages, V, and the price level at the residence location, P, per capita real earnings are defined as:

$$E_r^j = \left(\sum_w V_w^j F_{r,w}^j / P_r^j\right) \Big/ \sum_w F_{r,w}^j, j$$
$$= \text{Baseline, Hurricane}. \quad (5)$$

We empirically model changes in commuting flows and wages as functions of the fractional capital stock losses at commuting households' residence tract origins and workplace tract destinations,

$$\hat{F}_{r,w} = \varphi^F(\kappa_r, \kappa_w) \text{ and } \hat{V}_w = \varphi^V(\kappa_r, \kappa_w) \quad (6)$$

and impute changes in local price levels using the equilibrium conditions of the labor market (see appendix). These results are integrated into equations (5) and (6), which we numerically parameterize using LODES data for 2019 and combine with tract-level fractional capital stock losses to estimate labor losses via equation (4).

3. Results

3.1. Hurricane hazards, assets and societal exposures

Figure 1 panels (A)–(D) summarize the intensity of hurricane hazards, illustrating the expected and worst-case surge inundation depths and peak wind gust speeds for 97 hurricane events at property locations. Properties prone to flooding (>0.6 ft) are along the coasts and estuaries, especially New Hanover, Pender, and Brunswick counties. Wind impacts a broader area, with terrain slowing wind speeds inland away from the coastline. The most intense hurricane (figure A1, panel (A), thick line) makes landfall in New Hanover county traveling north, exposing New Hanover, Pender, and Onslow counties to >6 ft surge flooding and >180 mph wind gusts. Relatively high property values in New Hanover, Bladen, Wake, Currituck, and Dare counties (panel (E)) highlight these areas' potential for larger economic losses from structural damage.

3.2. Property losses

Figure 2 panels (A)–(F) summarize expected and worst-case property-level losses from wind, flood, and total combined structure and content damages. Exposed coastal properties in New Hanover, Pender, and Onslow counties experience the largest flood damage and loss, both in expectation and the worst case (panels (A) and (B)). The entire region is subject to wind damage, with expected losses concentrated

[6] The SVI is constructed by calculating the tract percentile ranks for each of the 16 variables, summing the ranks within each theme and ranking the resulting sums, and finally summing the four theme ranks and ranking the overall sum.

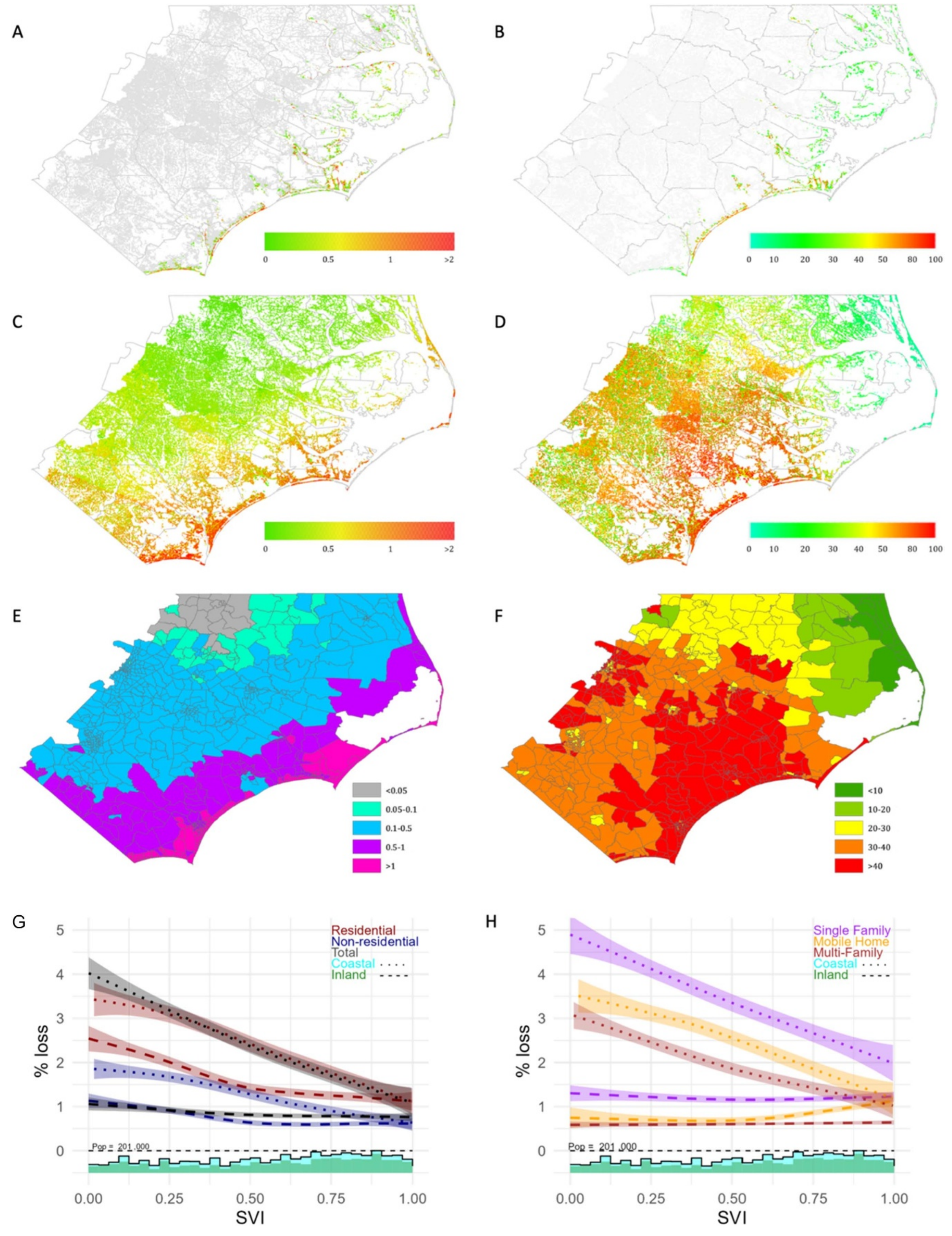

Figure 2. Hurricane surge, wind and total damage (percent of structure and content value). (A), (B) Property-level expected and worst-case storm surge damage. (C), (D) Property-level expected and worst-case wind damage. (E), (F) Census tract-level expected and worst-case total damage. (G), (H) Smoothed probability-weighted variation of % losses with SVI, coastal (dotted) and inland (dashed) census tracts.

along the southeast and eastern coasts, followed by the southwest and middle regions, and the smallest losses in the inland northwest (panel (C)). For the worst-case event, losses exceed 80% of the total values of properties in the vicinity of the south-to-north track, and decline longitudinally outward from that locus (panel (D)). Expected aggregate losses (panel (E)) exceed 0.5% (1%) of the total value of structures and their contents in census tracts in coastal regions (figure A2, panel (A)), especially New Hanover, Brunswick, Pender, and Carteret counties. The worst-case storm incurs huge capital losses in Cape Fear and along the entire Eastern Carolina coast, exceeding 40% of the total exposed property value (panel (F)).

Our main result is shown in panels (G) and (H): in coastal regions (figure A2, panel (A)), tract-level total losses decrease with SVI, an effect that is

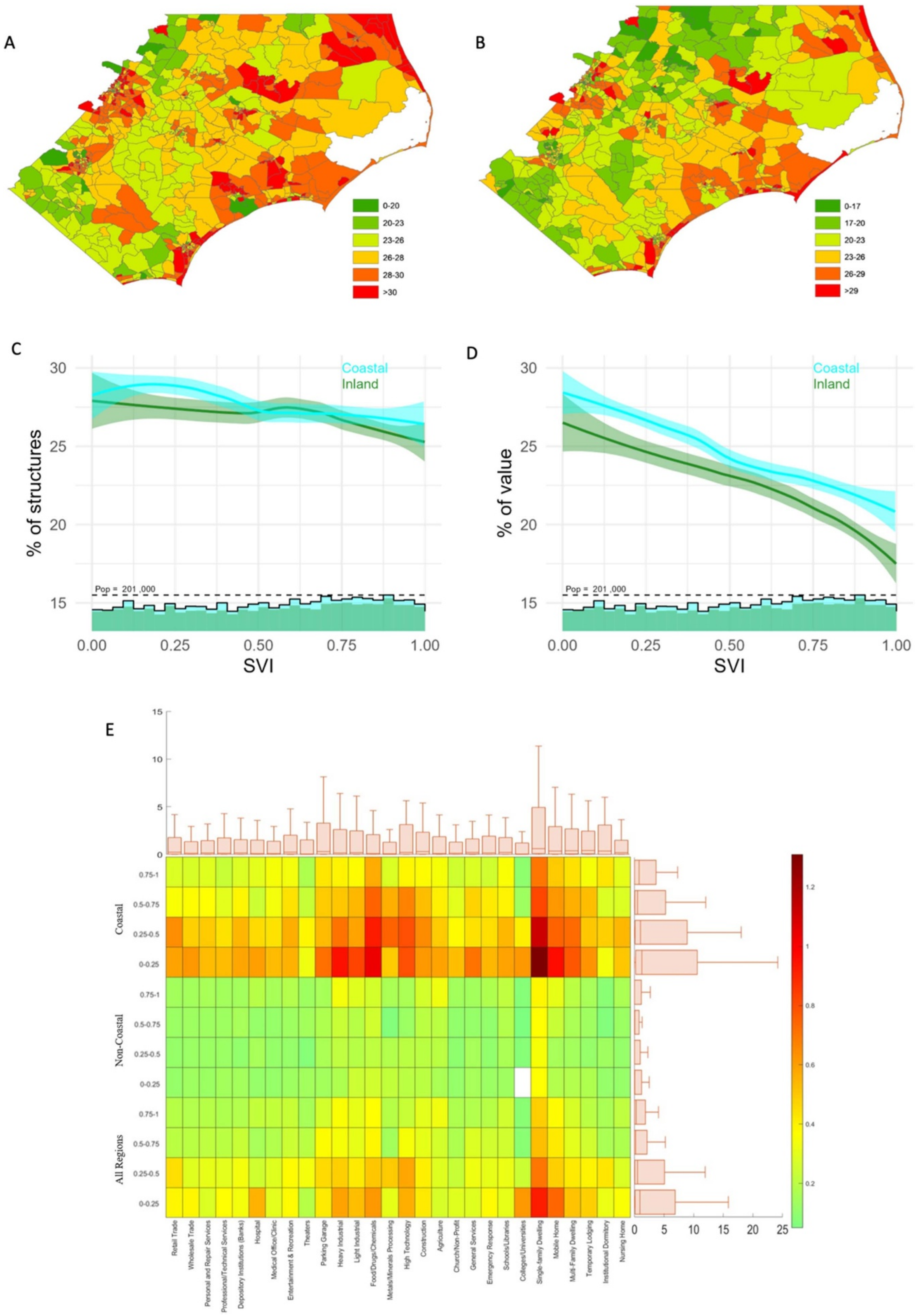

Figure 3. Census tract damage exposure of buildings and building values, and regional losses. (A), (B) Expected percentage of structures and total structure and content value with expected non-zero damage. (C), (D) Smoothed variation of probability-weighted % of affected structures and value with SVI, coastal (cyan) and inland (green) census tracts. (E) Expected percentage loss by region, social vulnerability index quartile, and Hazus occupancy class. Regions as in figure (B).

concentrated in residential occupancy classes, which reflects vulnerable households' propensity to locate inland, away from coastal amenities and associated high housing values and costs. There is no similar relationship inland, except for easily wind-damaged mobile homes.

Figure 3 provides further elaboration. Across both coastal and inland census tracts, the fraction

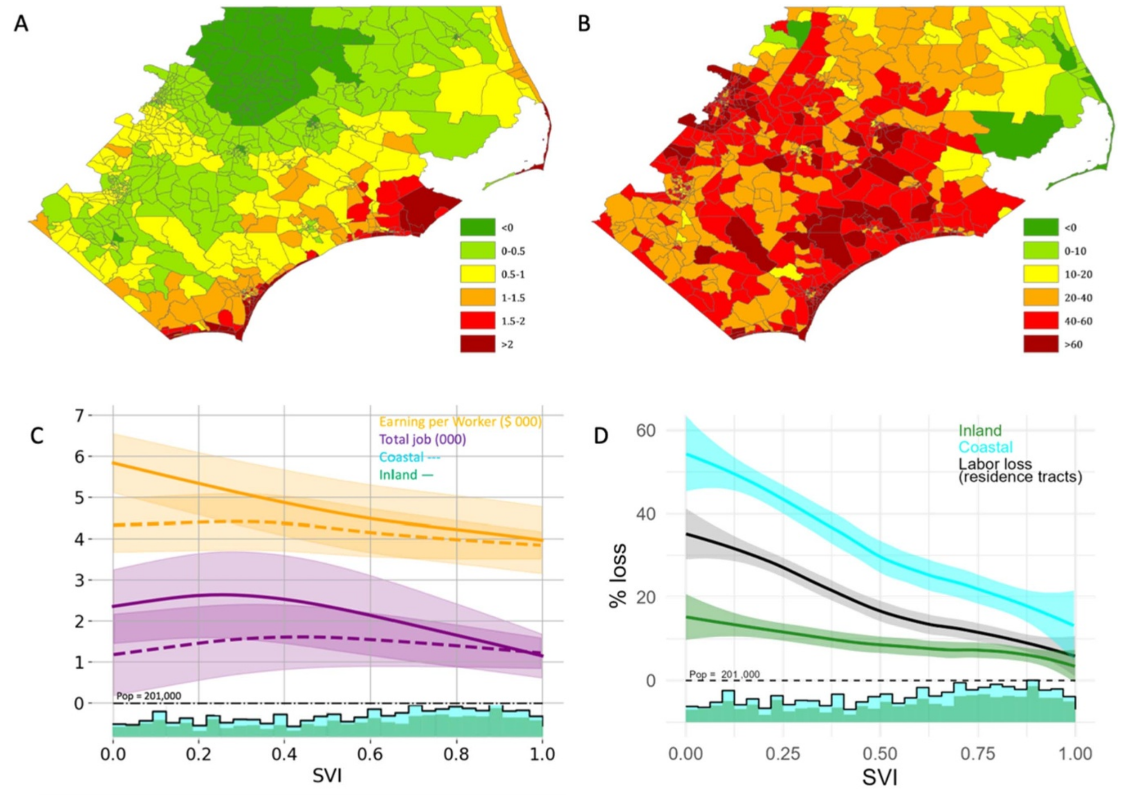

Figure 4. Labor losses (percent of value of earnings). (A), (B) Expected and worst case losses by residence census tracts. (C) Smoothed variation of total jobs and monthly earnings ($'000) by place of residence. (D) Probability-weighted % losses with SVI, all (black), coastal (blue) and inland (green) census tracts.

of structures sustaining non-zero damage is largely invariant to SVI (panels (A) and (C)), which is inconsistent with the hypothesis that more vulnerable households face systematically larger hazard exposures. Conversely, the fraction of tracts' structure and content value that sustains non-zero damage declines strongly with SVI (panels (B) and (D)), consistent with the hypothesis that the value of exposed assets is the major driver of overall losses. The upshot is that coastal regions incur much larger losses across a range of occupancy classes (panel (E)), which reach as high as 23% in the least socially vulnerable census tracts. Industrial and residential sectors bear the brunt of losses, up to 12% for single-family homes. Inland, losses are smaller and evenly distributed across sectors and tracts of different vulnerability. Across sectors and individual counties, the bulk of losses is driven by damage from wind as opposed to surge (figure A5).

3.3. Labor losses

Figure 4 summarizes the labor losses. Panels (A) and (B) present the spatial distribution of the expected and worst-case labor losses at the census tract level. The expected labor losses are declining along a southeast-to-northwest axis: counties such as New Hanover, Brunswick, Pender, and Carteret suffer the most significant labor losses, with values exceeding 1%, while counties like Franklin, Halifax, Nash, and Warren realize positive labor earnings due to residents can commute to affected areas to earn higher wages. In the worst case, substantial labor losses are located near the hurricane's track, surpassing 40% in counties like New Hanover, Pender, Onslow, Duplin, and Wake, and decay with distance from the track. Comparing figure 4 with figure 2, we also find distinct differences between labor and capital losses, indicating the significant redistribution effect caused by commuting households. Panel (C) shows the distribution of wages and jobs by residence tract in the baseline case. Panel (D) presents the calculated labor losses increase as the SVI falls. This relationship holds in both coastal and inland tracts and is more salient in coastal tracts.

4. Discussion and conclusions

We have combined detailed wind and surge hazards for 97 storms representative of eastern NC's hurricane climatology, property-level on the characteristics and values of residential and nonresidential structures and their values, and structure-matched wind and flood damage functions to estimate community-scale expected and worst-case hurricane losses. We further analyzed the implications of property damage at workers' census tracts of employment and residence for labor losses.

Table 1. Capital and labor losses by region (million 2021 $). Main estimate is the expected value for the 97-storm set, inter-quartile range shown in square braces.

	Capital stock losses					
	Residential	Commercial	Industrial	Other	Total	Labor Losses
Triangle J	298.9 [11.5, 506.2]	41.0 [0, 44.5]	17.6 [0, 22.4]	17.3 [0, 22.9]	374.8 [11.5, 578.1]	80.0 [17.5, 152.0]
Kerr-Tar	7.2 [0.5, 21.3]	1.0 [0, 1.8]	1.1 [0, 2.1]	0.5 [0, 1.4]	9.7 [0.5, 27.2]	−1.1 [−5.5, −4.5]
Upper Coastal Plain	36.2 [3, 124.5]	9.5 [0, 20.5]	6.2 [0, 13.9]	4.1 [0, 12.8]	56.0 [3, 173.6]	−21.5 [−81.3, −75.8]
Mid-Carolina	209.0 [4.3, 353.2]	58.5 [0, 61]	14.9 [0, 22.6]	19.5 [0, 32.9]	301.8 [4.3, 469.8]	40.3 [26.7, 58.1]
Lumber River	125.1 [1.6, 143.1]	38.8 [0, 21.8]	34.3 [0, 31.1]	24.2 [0, 22.9]	222.4 [1.6, 216.2]	16.9 [−9.8, 2.6]
Cape Fear	879.8 [9, 4377.6]	178.4 [0, 748.8]	61.6 [0, 251.7]	47.9 [0, 187.5]	1167.7 [9, 5701.1]	137.9 [87.9, 728.7]
Eastern Carolina	532.8 [34.2, 5190.1]	121.4 [3.6, 1205.8]	38.4 [0.7, 389.3]	40.1 [0.7, 351.9]	732.8 [38.9, 7177.5]	78.4 [56.3, 607.9]
Mid-East	81.3 [6.2, 474.1]	16.2 [0.1, 81.3]	7.4 [0, 42.4]	6.0 [0, 36.3]	111.0 [6.4, 638.5]	13.0 [−1.0, 53.5]
Albermarle	151.1 [19.3, 601.8]	24.9 [4.2, 118.4]	6.6 [1.9, 38.2]	7.2 [1.5, 40.2]	189.9 [28.9, 794.5]	16.5 [11.7, 70.1]
Study Region	2321.4 [89.7, 11 792]	489.8 [8, 2303.8]	188.2 [2.6, 813.7]	166.8 [2.2, 708.8]	3166.2 [104.2, 15 776.5]	431.2 [129.8, 3020.8]

As summarized in table 1, the expected value of damage to structures and their contents exceeds $3 Bn, 60% of which is incurred by coastal regions (Cape Fear and Eastern Carolina), and 70% of which is accounted for by residential buildings. Losses are heavy-tailed (Pollack *et al* 2022). For capital losses ranked across storm events, expected damage exceeds the 25th percentile by a factor of 30 and is in turn one-fifth of the 75th percentile. Annual labor losses are about one-seventh of capital stock losses, follow similar regional patterns and across storms are less strongly skewed. Regarding the paper's motivating question, both categories of losses decline with the social vulnerability of affected areas. This phenomenon manifests despite much weaker relationships between the SVI and either the total stock of buildings subject to hurricane damage, or total jobs and earnings per worker, which we attribute to the inverse relationship between SVI and households' income and the values of their own and the encompassing community's assets. In summary, two key conclusions can be drawn from our analysis of property and labor: (1) there is a sustainable difference between capital and labor losses, with capital losses predominating, and (2) both types of losses increase when the SVI decreases, across both coastal and inland regions.

An advantage of our bottom-up approach is in pinpointing 'outlier' communities that are both socially vulnerable and disproportionately exposed to hurricane losses. Among census tracts with >80th percentile SVI scores, those with expected labor losses exceeding 1.5% of annual earnings include Shallotte (206.01), Morehead City (705.01), Hatteras Island (705.02), and Wilmington (103, 108, 111), and those with expected capital losses exceeding 20% of aggregate structure and content values include Leland (201.01), Myrtle Head (206.01), Bolton (302), Hatteras Island (705.02), Wilmington (103, 108, 110, 111) and Highsmith (601). Such information is crucial for implementing mitigation and adaptation policies' goal of allocating resources to communities most 'at risk' and 'in need'. Even so, our main result suggests that additional metrics may be needed to capture impacts on marginalized/vulnerable populations that own low-value assets, and for whom small absolute losses likely mask substantial risks to their livelihoods and well-being.

While there are only a few prior studies against which our results can be contrasted, their total losses lie within the interquartile range of our estimates. In ESP's (2021) analysis of building vulnerabilities to 100y return period hurricane winds across southeastern NC (Brunswick, New Hanover, Onslow, and Pender counties), aggregate property losses reach \$6 Bn. Similarly, Mazumder *et al* (2023) analyze damage to buildings in Onslow county from hurricane Helene-1958 and five derivative synthetic storms, and estimate losses totaling \$5.5–\$9.5 Bn. Similar to the present work, FEMA Hazus Loss Library's (FEMA 2023) 20y retrospective analyses of NC cyclones estimates substantial economic costs—\$2.4 Bn and \$1.2 Bn for hurricanes Florence and Isabel, and \$1.2 M and \$3.5 M for hurricanes Alex and Ivan, whose impacts are more localized. At the tract level, the event-specific capital exposures and losses are negatively correlated with social vulnerability, generally corroborating our main result (table A2).

Notwithstanding, our findings are subject to multiple caveats. Perhaps most consequential is the potential limitations of our wind model (Holland 1980) relative to newer parametric schemes (e.g. Chavas *et al* 2015, Chavas and Lin 2016) that adjust the radial structure of cyclone wind fields, or high-resolution dynamical simulations (e.g. Rotunno *et al* 2009, Wu *et al* 2018) that resolve $<$10 km-scale high wind streaks (Hendricks *et al* 2021, Nolan *et al* 2021a, 2021b) or $\sim$100 m scale coherent eddies (so-called tornado-scale vortices—Wu *et al* 2018, Liu *et al* 2021, 2022) that are embedded in, and locally enhance peak wind gusts and damage associated with, the broader cyclonic flow (Wurman and Kosiba 2018, Sanchez Gomez *et al* 2023). Notwithstanding, methods to translate burgeoning scientific insights from these alternatives into new methods for operational risk analysis are still in their infancy (e.g., Stern *et al* 2021, Wang *et al* 2022), and are fraught with uncertainties regarding the precise location and magnitude of gust enhancement as storms' characteristics interact with their onshore boundary layer environment.

Additionally, our focus on wind and storm surge does not account for damage and losses that can extend far inland due to precipitation-driven increases in river flows into coastal areas (fluvial flooding) and water accumulation on land (pluvial flooding). Capturing the fluvial component requires a multi-model system that includes a hydrological/hydraulic model to route water into coastal rivers, and provide additional boundary conditions for ADCIRC (e.g. Dresback *et al* 2013, Blanton *et al* 2018, Davidson *et al* 2018). Such coupling is essential to capture potential interactions between rainfall- and surge-related inundation that can generate hurricane-driven compound flooding (Wahl *et al* 2015, Gori *et al* 2020, Zhang *et al* 2020). However, modeling the spatial and temporal evolution of hurricane-related precipitation fields remains a key challenge, and the state of the art is rapidly evolving (Brackins and Kalyanapu 2020, Gori *et al* 2020, Nakamura *et al* 2024, Vosper *et al* 2023, Yang *et al* 2023).

The foregoing considerations suggest that true damages likely exceed those shown in table 1, especially in non-coastal areas. But an open question is the extent to which incorporating high-resolution wind modeling and/or inland flooding could alter the relationship between SVI and losses. Additional losses depend on the uncertain distribution of tornadic wind and inundation hazards and their interaction over space with depth-damage functions whose slope depends on affected structures' attributes, further modulated by the max() function in equation (1). These issues are ripe for investigation.

A second limitation stems from the simplified nature of Hazus' damage functions, particularly for flooding. The shapes of depth-damage relationships are not strongly modulated by structural attributes. Moreover, limited information on such characteristics in the NSI often necessitated assignment of averaged damage functions to individual buildings. Potential biases that attend these modeling choices can mischaracterize true building-level losses, but establishing the magnitude of over- or underestimation requires comparisons with more sophisticated structural engineering models (e.g. Nofal *et al* 2021)—an effort that is well beyond the scope of the present study. The threat to our inference is that biases obscure the consequences of sorting of vulnerable households into less hurricane-resistant, more damage-susceptible structures, and the true SVI-loss relationship. Notwithstanding, such errors are likely at least partially mitigated by the high spatial resolution of our building inventory—notwithstanding the unavoidable coarseness of our wind hazards (Pollack *et al* 2022).

Third, our analysis is static, treating hurricanes as independent discrete events and capital damage as immediate losses to which labor losses are directly tied. In reality, labor losses will depend on the dynamics of recovery and endogenous labor market responses to them. We do not account for the impact of residence or workplace damage on migration or business interruption that trigger separation of workers from their pre-storm jobs, which can account for almost all of the decline in earnings in the first-year post-storm (Groen *et al* 2020). Intertemporal losses can be mitigated by faster resumption of business activity and hiring, and restoration of transportation lifelines that connect residences and employers (Sue Wing *et al* 2023). Symmetrically, they can be amplified by damage from successive hurricane events that occur before the economy has had a chance to fully recover, prolonging business interruption, housing insecurity and unemployment.

We close by briefly outlining next steps. Ongoing research by the authors and their collaborators seeks to describe more comprehensively the fluvial, pluvial and compound flooding components of hurricane hazards. Our strategy extends Blanton *et al's* (2018) coupled modeling system to incorporate a parametric rainfall model and a larger suite of storm events from a recent stochastic tropical storm dataset (Bloemendaal *et al* 2020). We anticipate that the resulting hazard information, in conjunction with improvements to the bottom-up loss methodology presented here, will yield more detailed and complete assessments of economic losses, and further elucidate interactions between hurricane hazards, the built environment, and human behavior.

Data availability statement

The data cannot be made publicly available upon publication because the cost of preparing, depositing and hosting the data would be prohibitive within the terms of this research project. The data that support the findings of this study are available upon reasonable request from the authors.

Acknowledgement

This research was supported by National Science Foundation grant no. 2209190.

Appendix

A1. Social vulnerability and its measurement

As outlined by the CDC/ATSDR (2020), it is crucial for communities to prepare for the challenges posed by natural hazards. However, many social factors, known as social vulnerability, can significantly impact a community's ability to minimize economic losses from such disasters. These factors include, but are not limited to, poverty, crowding, and age demographics. Cutter *et al* (2003) initially constructed an index of social vulnerability (SVI) at the county level to effectively assess and rank social vulnerability based on 11 independent factors. Following this approach, the CDC/ATSDR created their own version of the SVI for the entire United States at the census tract level, with the most recent update being in 2020.

As discussed in the main text, this study employs the CDC/ATSDR's SVI, which is calculated using 4 key themes that encompass 16 different variables. These themes are Socioeconomic Status, Household Composition and Disability, Minority Status and Language, and Housing and Transportation. Table A1.1 provided below details the specific variables categorized under these themes (CDC/ATSDR 2020). As mentioned in the footnote of the main text, the SVI is constructed by calculating the tract percentile ranks for each of the 16 variables, summing the ranks within each theme and ranking the resulting sums, and finally summing the four theme ranks and ranking the overall sum.

Table A1.1. Themes and variables of social vulnerable index.

Themes	Variables
Socioeconomic status	Below 150% poverty Unemployed Housing cost burden No high school diploma No health insurance
Household characteristics	Aged 65 & older Aged 17 & younger Civilian with a disability Single-parent households English language proficiency
Racial and ethnic minority status	Race
Housing type and transportation	Multi-unit structures Mobile homes Crowding No vehicle Group quarters

A2. Flood and wind damage functions

FEMA's Hazus model is a highly effective tool for analyzing risks of natural hazards, including a comprehensive suite of damage and loss functions specifically designed for accurate loss estimation. This study utilizes these pre-established functions to conduct our damage and loss calculations.

A2.1. Flood

The Hazus flood model (FEMA 2022b) offers an array of flood damage loss functions for both structures and contents, elaborated in sections 5 and 6, specifically in tables 5–2, 5–3, 5–4, 6–1, and 6–2. These functions delineate the relationship between flood depths (measured in feet) and the percentage damage losses across various building occupancies. Given our paper's focus on surge flooding resulting from hurricanes, we selectively applied functions suited for coastal regions. As previously discussed, our study encompasses 28 occupancy classes, with each class assigned a specific damage loss function. To enhance the precision of damage loss calculations, the category 'RES1' (single-family residences) is further subdivided into 8 groups based on the number of stories and the presence of basements, leading to a total of 35 functions for flood loss assessment (illustrated in table A1 column 'Flood' and figure A3). Notably, the functions related to the eight subcategories of 'RES1' are originally derived from the Federal Insurance Administration, while the functions for the remaining 27 occupancy categories originate from the U.S. Army Corps of Engineers, Galveston District (USACE-Galveston). It is important to mention that the flood functions utilized are extracted from the Hazus database.

A2.2. Wind

The Hazus hurricane model (FEMA 2022a) offers a comprehensive array of wind damage loss functions for structures and contents, detailed in sections 5 and 8. Unlike flood-related functions, the wind damage functions account for a variety of critical factors, including terrains and the structural resistance of buildings, among others. Specifically, a building's resistance is determined by a combination of several characteristics such as the roof, walls, connections, windows, etc, leading to plenty of different wind functions for estimating potential damages and losses. Overall, Hazus has compiled a comprehensive set of wind damage loss functions in its database, each considering different resistances, building types, and terrains.

To facilitate analysis, Hazus has categorized these wind functions based on defined hurricane-specific building types, as outlined in table 4–4 within section 4 (FEMA 2022c). This classification considers factors such as building types, occupancy classes, the number of stories, construction year, and other relevant details. Our study classifies buildings within the NSI according to these 39 hurricane-specific building types. We then average the functions associated with each type, drawn from the Hazus database, to represent the damage and loss function for that category. As a result, this research incorporates a total of 39 wind functions, featured in the 'Wind' column of table A1 and visualized in figure A4, for assessing both structural and content-related damages and losses. These functions illustrate the relationship between gust wind speeds and the percentage of damages and losses.

A3. Labor losses

A3.1. Empirical Analysis

In this section, we use historical data to characterize the impacts of hurricane-driven capital stock destruction on commuting flows and wages.

Our proxies for capital losses are taken from the Hazus Loss Library. To compute fractional losses suffered by residence and workplace census tracts, κ_r and κ_w, we divide estimated damage to building and content stocks by the total exposed value of these stocks. We include all recorded hurricanes affecting NC from 2003–2018, 15 events in total, which we aggregate to an annual time step by computing the ratio of total annual damage to the value of the stock. We do not extend our historical dataset beyond 2019 to avoid the severe confounding labor market effects of the COVID-19 pandemic.

We first quantify the impact of hurricanes on commuting flows. We restrict the universe of NC census tracts to the subset that experience any hurricane-driven capital stock losses over the study period, and construct the matching subset of LODES commuting flows for which affected tracts are origins, destinations, or both. The result is a list of tract dyads linked by historically observed commuting, from which we filter entries with cumulative flows <30 workers over the study period, for a final sample of 83 625 tract pairs.

Our empirical model of residence-workplace flows is the gravity model:

$$\begin{aligned}\tilde{F}_{r,w,t} = \xi^F + \rho^F \tilde{F}_{r,w,t-1} + \beta_1^F \tilde{L}_{w,t-1} + \beta_2^F \tilde{N}_{r,t-1} \\ + \gamma_1^F \log V_{r,t-1} + \gamma_2^F \log V_{w,t-1} + \delta_1^F \kappa_{w,t-1} \\ + \delta_2^F \kappa_{r,t-1} + X_{r,w}^F \eta^F + \mu_{r,w}^F + \tau_t^F + \varepsilon_{r,w,t}^F\end{aligned} \tag{A3.1.1}$$

where t indexes years, $F_{r,w}$ is the flow of workers from residence tract to workplace tract w, L_w and N_r denote total employment in workplace tracts and total working population in residence tracts, and V and κ denote wages and fractional capital losses at origin and destination tracts. We control for unobserved geographically-varying time-invariant confounders by including tract-pair fixed effects, μ^F, for time-varying common shocks by including year fixed effects, τ^F, and we include additional dummy controls associated with tracts' metropolitan statistical area, X^F. A large fraction of tract pairs in our sample have zero commuting flows in any given year, which poses a challenge for estimation. To deal with this issue, we apply the inverse hyperbolic sine transformation to F, L, and H, indicated by a tilde over a variable. The latter enable the estimated parameters of interest (β^F, γ^F, δ^F) to be converted to elasticities or semi-elasticities (Bellemare and Wichman 2020). Finally, we cluster the standard errors at the tract-pair level.

Next, we quantify the hurricanes' impact on wages in workplace tracts. For tracts with non-zero employment, we estimate the following model:

$$\begin{aligned}\log V_{w,t} = \xi^V + \rho^V \log V_{w,t-1} + \beta^V \log L_{w,t-1} \\ + \delta^V \kappa_{w,t-1} + \eta^V X_w^V + \mu_w^V + \tau_t^V + \varepsilon_{w,t}^V.\end{aligned} \tag{A3.1.2}$$

Here, X^V is a dummy variable that equals one if the tract w is located in a metropolitan area and zero otherwise, while μ^V and τ^V denote tract fixed effects and year fixed effects that control for unobserved spatially-varying time-invariant confounders and time-varying common shocks, respectively. Standard errors are clustered at the tract level. We initially followed equation (6) and included as covariates loss ratios at workplaces (κ_w) as well as the compensation-weighted average loss ratios at the residence tract origins corresponding to each workplace ($\overline{\kappa}_w$). However, the two metrics were highly correlated due to the spatially contiguous damage from hurricanes' wind fields, which introduced severe multicollinearity into the regression. Accordingly, $\overline{\kappa}_w$ was dropped as a covariate in favor of our preferred specification shown in equation (A3.1.2).

The empirical results are presented in table A3.1.1. We find that hurricanes positively affect both

Table A3.1.1. Regression Results

Variables	Origin-destination flow	Wage at workplace
Lag of working population in workplace	0.451***	0.0454***
	(0.003 54)	(0.003 93)
Lag of working population in residence	0.466***	—
	(0.004 77)	—
Lag of wage in workplace	0.130***	0.452***
	(0.008 71)	(0.0114)
Lag of wage in residence	−0.0159	—
	(0.0126)	—
Capital loss ratio in workplace	3.080***	1.364***
	(1.134)	(0.485)
Capital loss ratio in residence	−0.913	—
	(1.058)	—
Constant	Yes	Yes
Lag of work flow	Yes	—
MSA control	Yes	Yes
Group fixed effect	Yes	Yes
Year fixed effect	Yes	Yes
Observations	1170 750	30 467
R-squared	0.166	0.548
Number of groups	83 625	2181

Note: Robust standard errors in parentheses. *** $p < 0.01$, ** $p < 0.05$, * $p < 0.1$.

commuting inflows and local wages of the affected tracts. These findings are consistent with previous literature arguing that more job opportunities will be created after hurricanes. The high labor demand increases wages and attracts more people to work in the affected areas. It is also worth noting that elasticities of capital losses on wages and workflows are large, indicating the phenomenal impacts of hurricanes on the local labor market in NC. However, higher wages and workflows do not necessarily indicate an improvement in welfare. There are at least two additional impacts to be quantified before any conclusions about welfare are made: (1) higher wages and more workers also indicate higher prices of goods, which would have a negative effect on the household's real income; (2) changes in the commuting workflow could lead to the redistribution of income, then who actually gets benefits from hurricanes becomes unclear. More sophisticated calculation is required to uncover the impact of hurricanes on the entire region.

A3.2. Welfare Analysis

Our approach is deliberately simple. We assume that in each census tract there is a representative producer that generates output of a final good, Q, with a local price, P, from quantities of labor (L) and capital (K) according to Cobb-Douglas production technology with capital-output elasticity, α,

$$Q_w = {K_w}^{\alpha_w} {L_w}^{1-\alpha_w}. \tag{A3.2.1}$$

The condition for short-run equilibrium in the labor market is equivalence of the real wage and the marginal product of labor:

$$V_w/P_w = (1-\alpha_w)\,{K_w}^{\alpha_w} {L_w}^{-\alpha_w} \tag{A3.2.2}$$

from which the price level can be recovered as:

$$P_w = (1-\alpha_w)^{-1} {K_w}^{-\alpha_w} {L_w}^{\alpha_w} V_w. \tag{A3.2.3}$$

Using a hat over a variable to indicate its logarithmic differential, or fractional change (e.g. $\hat{x} = \mathrm{d}\log(x) = \mathrm{d}x/x$), (A3.2.3) can be expressed in log-differential form. Noting that κ_w is simply the workplace capital loss computed in equation (3), the fractional change local price level is:

$$\hat{P}_w = \alpha_w \kappa_w + \alpha_w \hat{L}_w + \hat{V}_w. \tag{A3.2.4}$$

In each census tract, the final good is consumed by the households who reside there. Households' level of consumption is determined by the wage they receive and the price of the final good. However, households do not necessarily work in the census tract where they reside. In particular, a representative individual residing in residence tract, r, and working in workplace tract, w, will enjoy utility determined by the level of per capita real earnings, given in levels and fractional changes by (5) and (6) in the main text.

The immediate implication is that real income and welfare in any given location will depend on two separate effects. For households who both live and work in census tract j ($j = r = w$), equation (6) in conjunction with our empirical results suggest that hurricane-driven damage to the capital stock reduces real income and welfare: $\kappa_j > 0 \Rightarrow \hat{L}_j > 0 \Rightarrow \hat{E}_j < 0$. For households who live and work in different census tracts, $j = r \neq w$, our empirical results suggest that households are incentivized to work in locations with higher wages, and will switch jobs and workplaces in an attempt to adapt to hurricane shocks. The crucial implication is that changes real income and welfare in any given residence location will depend upon the magnitude of changes in commuting flows from that location and the changes in wages at those flows' workplace destinations, $F_{r,w}$.

The welfare impact on households residing in tract r can be approximated by the fractional change in per capita real earnings, or $LL_r(s) / \left(E_r^{\mathrm{Baseline}} \cdot N_r\right)$ by equation (4). Given that total employment at each workplace tract is $L_w = \sum_k F_{k,w}$, the welfare impact can be elaborated by log-differentiating equation (5) and using (A3.2.4) to eliminate the change in the price level:

$$
\begin{aligned}
\hat{E}_r &= \sum_w \theta_{r,w}\left(\hat{V}_w + \hat{F}_{r,w} - \hat{P}_r\right) - \sum_w \zeta_{r,w}\hat{F}_{r,w} \\
&= \sum_w \theta_{r,w}\hat{F}_{r,w} + \sum_w \theta_{r,w}\left(\hat{V}_w - \hat{V}_r - \alpha_r\kappa_r - \alpha_r\hat{L}_r\right) \\
&\quad - \sum_w \zeta_{r,w}\hat{F}_{r,w} \\
&= \sum_w \left(\theta_{r,w} - \zeta_{r,w}\right)\hat{F}_{r,w} \\
&\quad + \sum_w \theta_{r,w}\left(\hat{V}_w - \hat{V}_r - \alpha_r\kappa_r - \alpha_r\sum_k \omega_{k,r}\hat{F}_{k,r}\right) \\
&= -\alpha_r\kappa_r + \sum_w \theta_{r,w}\left(\hat{V}_w - \hat{V}_r\right) \\
&\quad + \sum_w \left(\theta_{r,w} - \zeta_{r,w}\right)\hat{F}_{r,w} - \alpha_r\sum_k \omega_{k,r}\hat{F}_{k,r}
\end{aligned}
\tag{A3.2.5}
$$

where $\zeta_{r,w} = F_{r,w}/\sum_k F_{r,k}$ and $\theta_{r,w} = F_{r,w}V_w/\sum_k F_{r,k}V_k$ denote the shares of each place of work in a particular residence tract's total working population and total earnings, respectively, and $\omega_{r,w} = F_{r,w}/L_w$ denotes the share of each place of residence in a particular workplace tract's total labor demand.

Equation (A3.2.5) decomposes hurricane-driven changes in earnings into four sources. The first term is the direct impact of capital stock destruction, the second is the effect of adjustments in relative wages, the third is the effect of worker adaptation due to switching workplaces, while the last is the impact of changes in worker inflows on wages earned by workers who are employed in the same tract in which they reside. The latter three indirect terms illustrate the importance of the commuting network's endogenous response to the spatial distribution of hurricane-driven physical destruction, with the potential to spatially redistribute the economic impacts of hurricane shocks. The differing signs of the effects highlights the fact that, from a theoretical standpoint, whether earnings increase or decline is undetermined. To address this question we turn to numerical simulation.

A3.3. Parameterization and Numerical Simulation

We numerically parameterize the algebraic model in section 2.2.1 and then quantify the welfare changes of the households living in the studied area using the simulated hurricanes. By equation (5), shocks to per capita real are driven by shifts in commuting flows, $F_{r,w}$, wages, V_w, and local prices, P_w. The series $F_{r,w}$ and V_w are estimated via the fitted regression equations (A3.1.1) and (A3.1.2), as follows. We take the year 2019 as our benchmark period, and impose the hypothetical simulated hurricane events with different occurrence probabilities as computed by Avipatanagul *et al* (2011).

Our first step is to estimate baseline commuting flows and wages in the absence of hurricanes. We compute these by combining the fitted equations (A3.1.1) and (A3.1.2) with values for L, N, V and F for 2019 in the LODES dataset, excluding the terms that capture the effects of hurricane-driven capital losses on commuting and wage outcomes:

$$
\begin{aligned}
\tilde{F}_{r,w}^{\text{Baseline}} &= \hat{\hat{\xi}}^F + \hat{\hat{\rho}}^F\tilde{F}_{r,w} + \hat{\hat{\beta}}_1^F\tilde{L}_w + \hat{\hat{\beta}}_2^F\tilde{N}_r + \hat{\hat{\gamma}}_1^F\log V_r \\
&\quad + \hat{\hat{\gamma}}_2^F\log V_w + X_{r,w}^F\hat{\hat{\eta}}^F + \hat{\hat{\mu}}_{r,w}^F
\end{aligned}
\tag{A3.3.1}
$$

$$
\begin{aligned}
\log V_w^{\text{Baseline}} &= \hat{\hat{\xi}}^V + \hat{\hat{\rho}}^V\log V_w + \hat{\hat{\beta}}^V\log L_w \\
&\quad + \hat{\hat{\eta}}^V X_w^V + \hat{\hat{\mu}}_w^V
\end{aligned}
\tag{A3.3.2}
$$

where a double hat indicates fitted values.

Our second step is to calculate the tract-level capital loss ratio for each simulated hurricane event $\kappa(s)$, following section 2.2.1, from which we estimate counterfactual with-hurricane commuting flows and wages:

$$
\tilde{F}_{r,w}^{\text{Hurricane}}(s) = \tilde{F}_{r,w}^{\text{Baseline}} + \hat{\hat{\delta}}_1^F\kappa_w(s) + \hat{\hat{\delta}}_2^F\kappa_r(s)
\tag{A3.3.3}
$$

$$
\log V_w^{\text{Hurricane}}(s) = \log V_w^{\text{Baseline}} + \hat{\hat{\delta}}_1^V\kappa_w(s).
\tag{A3.3.4}
$$

Our third step is to use (A3.2.2) to estimate P_w in the baseline and counterfactual scenarios. To accomplish this, at each workplace tract, aggregate labor is computed as: $L_w^{\text{Baseline}} = \sum_k \sinh\left(\tilde{F}_{k,w}^{\text{Baseline}}\right)$ and $L_w^{\text{Hurricane}}(s) = \sum_k sinh\left(\tilde{F}_{k,w}^{\text{Hurricane}}(s)\right)$, aggregate capital is calculated in the baseline by aggregating the value of properties the NSI, $K_w^{\text{Baseline}} = \sum_{i\in w} v_i$, and in the counterfactual scenario by $K_w^{\text{Hurricane}}(s) = K_w^{\text{Baseline}}(1 - \kappa_w(s))$. We calculate tract level capital income share, α_w, using 2019 IMPLAN accounts (IMPLAN® 2019) for NC, from which we obtain the labor shares of producers' factor input, $\mathcal{A}_c$, in the counties, c, in our study area. Recognizing that the ratio of capital and labor income shares at the county level is simply constituent tracts' aggregate value of labor compensation divided by the corresponding aggregate value of capital remuneration, the Implan data facilitate calculation of the county-level average rates of return on capital, ROR_c, as:

$$
\text{ROR}_c = \frac{\mathcal{A}_c}{1 - \mathcal{A}_c}\frac{\sum_{w(c)} V_w L_w}{\sum_{w(c)} K_w}.
\tag{A3.3.5}
$$

The further assumption that tract-level markets for capital result in rates of return that are identical and equal to the average of the encompassing county allows tract-level labor share parameters, α_w, to be recovered as:

$$
\alpha_w = \frac{V_{w(c)}L_{w(c)}}{V_{w(c)}L_{w(c)} + \text{ROR}_c K_{w(c)}}.
\tag{A3.3.6}
$$

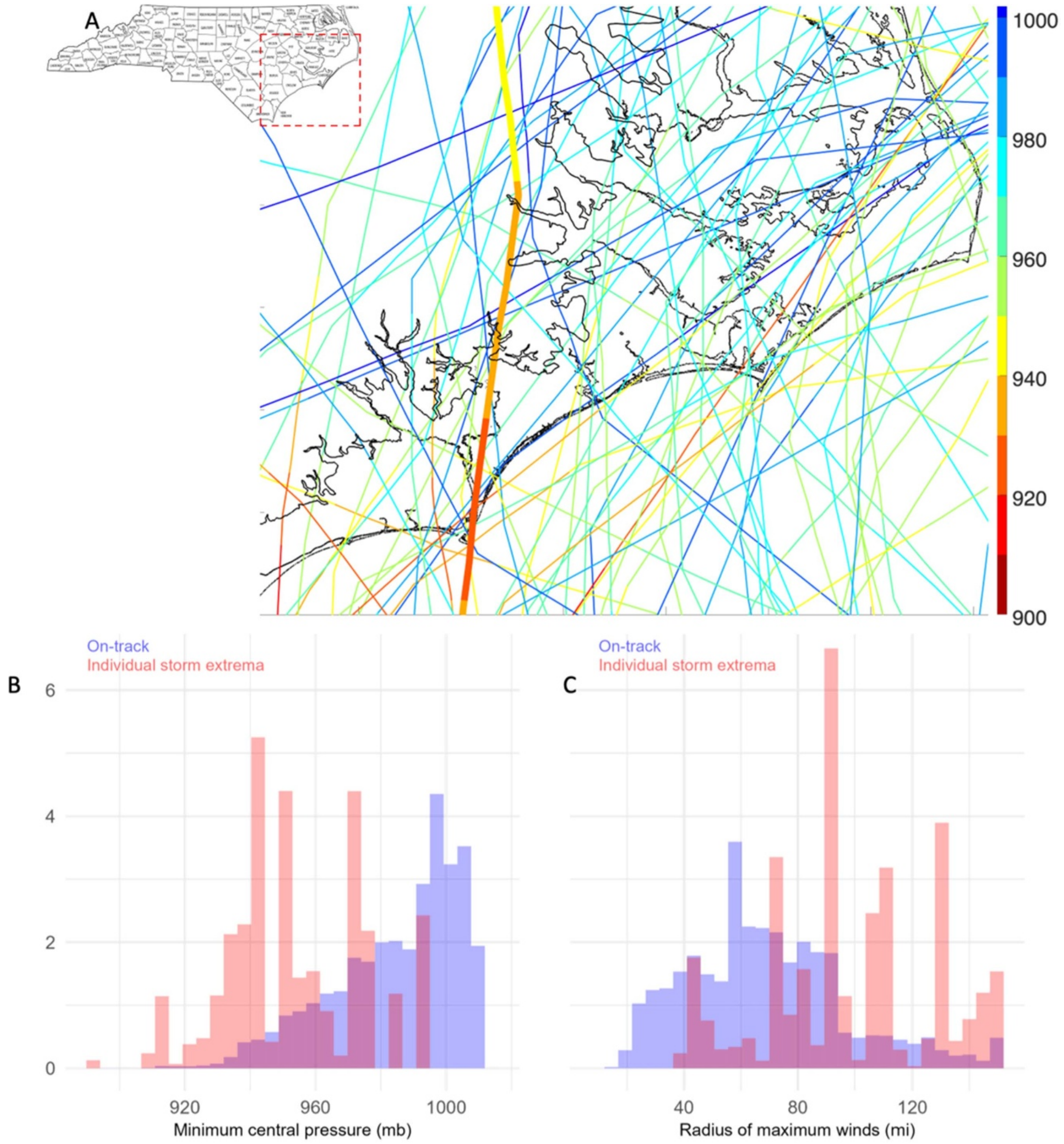

Figure A1. (A) Hurricane tracks colored by minimum central pressure (mb), worst-case storm shown in bold. (B), (C) Distributions of most extreme and on-track minimum central pressures and radii of maximum winds for the 97 hurricane set.

Local price levels in the baseline and counterfactual scenarios can then be calculated by plugging the corresponding input values into the right-hand side of (A3.2.3).

The resulting values of price levels, wages, and commuting flows permit equation (5) to be evaluated in the baseline and counterfactual hurricane scenarios:

$$E_r^{\text{Baseline}} = \left(\sum_w V_w^{\text{Baseline}} F_{r,w}^{\text{Baseline}} / P_r^{\text{Baseline}}\right) / \sum_w F_{r,w}^{\text{Baseline}} \tag{A3.3.7}$$

$$E_r^{\text{Hurricane}}(s) = \left(\sum_w V_w^{\text{Hurricane}}(s) F_{r,w}^{\text{Hurricane}}(s) / \times P_r^{\text{Hurricane}}(s)\right) / \sum_w F_{r,w}^{\text{Hurricane}}(s) \tag{A3.3.8}$$

in turn facilitating calculation of percentage and total labor losses as $E_r^{\text{Hurricane}}(s)/E_r^{\text{Baseline}} - 1$ and equation (4).

A4. Additional Explanations for the Results

Panels (A) and (B) in figure 2 provide a detailed visualization of surge flood damages to buildings across different scenarios. Panel (A) focuses on expected damages, highlighting significant impacts in coastal regions like Cape Fear and Eastern Carolina, where numerous buildings are projected to sustain damages of 1% or more. The color gray represents buildings with 0% damage, indicating no impact from flooding. Panel (B) examines a worst-case scenario where an extreme hurricane hits New Hanover County and tracks northward, causing substantial damage,

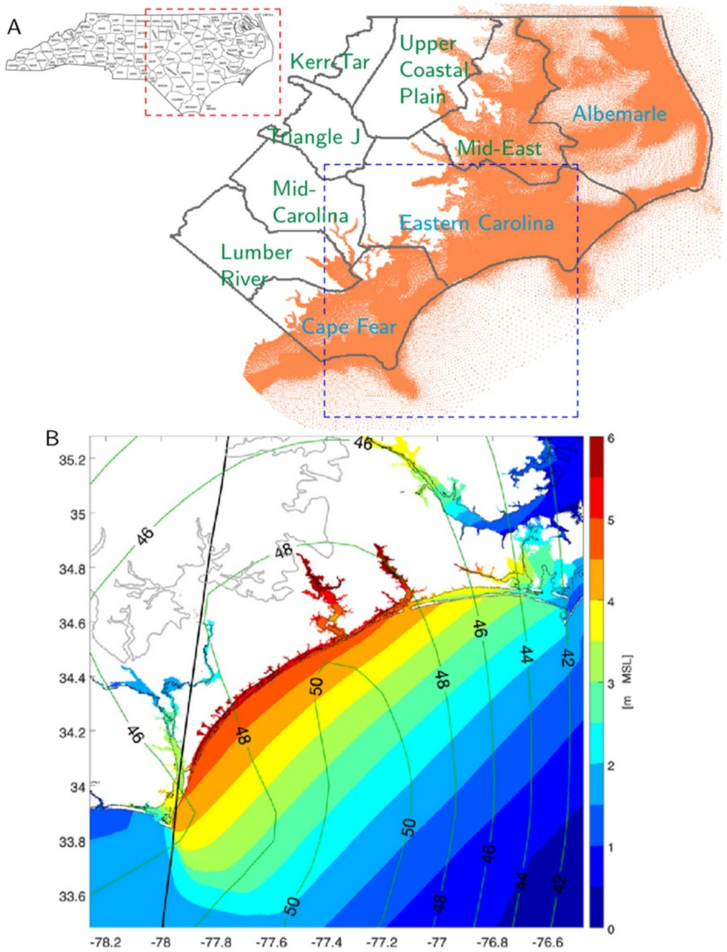

Figure A2. (A) 44-county CAMA study area showing ADCIRC grid, major regions (coastal: name in blue, inland: name in green), and inset for panel (B) (dashed blue). (B) Storm surge above mean sea level (color surface) and wind speed in m/s (contours) for the most intense hurricane in the 97-member storm set (track indicated by the thick black line). The coastline indicates mean sea level; water levels inland of that line represent overland inundation. Note the highest water levels are up the two estuaries, and in the land area in the northeast corner of the figure, indicating substantial inundation in these locations.

particularly in New Hanover County, Pender County, and southern Onslow County, where buildings could suffer over 80% flood damage. Conversely, coastal areas in the northeastern part of the state are estimated only to face around 10% damage.

Panels (C) and (D) in figure 2 shift the concentration to wind-related damages. In panel (C), under expected conditions, the southeast regions, notably Cape Fear and Eastern Carolina, could endure wind damage to buildings exceeding 1% or 2%. In contrast, the southwest and central regions are likely to experience lower wind damage, approximately 0.6%, while the northern regions might see negligible damage, close to 0%, due to milder hurricane effects. Panel (D) explores the severe hurricane scenario, where buildings not directly in the hurricane's path are estimated to incur relatively lower wind damage about 30%–50% compared to those on the path, and those in northeastern areas would experience minimal impact, around 0%. Panels (E) and (F) aggregate capital losses at the census tract level, showing patterns consistent with those observed in the individual building analyses.

Furthermore, panels (G) and (H) of figure 2 explore the relationship between losses and the SVI. For residential occupancies, losses decrease as SVI increases, where coastal areas indicate a reduction from 3% to 1.2% and inland areas from 2.5% to 1.2%, as SVI goes from 0 to 1. Non-residential occupancies exhibit a similar but less obvious trend, a decrease from 1.8% to 0.7% in coastal areas and from 1.1% to 0.7% in inland areas. Notably, single-family homes face the highest losses, followed by mobile homes and multi-family units, regardless of SVI. Coastal losses for these groups decline from 4.9%, 3.5%, and 3% to 2%, 1.2%, and 1%, respectively, with increasing SVI. Inland, single-family and multi-family losses remain stable across SVI levels at 1.3% and 0.6%, respectively. However, mobile homes show a unique opposite pattern where losses increase with SVI, moving from 0.7% to 1.2%.

Panels (A) and (B) in figure 3 highlight the percentage of buildings and total values experiencing expected non-zero damages across various census tracts. In particular, numerous tracts along the southeast, middle, and northeast coastal areas report that

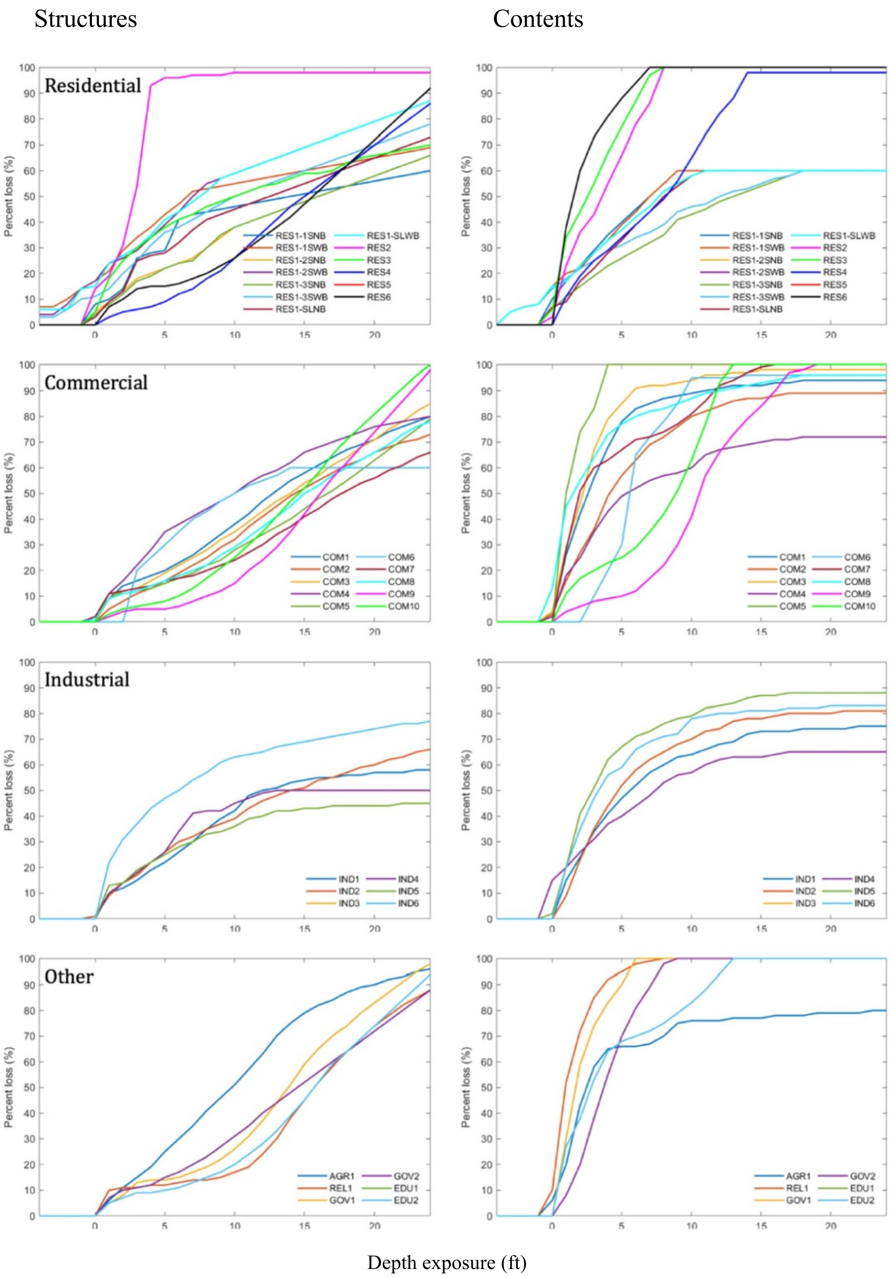

Figure A3. Hazus sectoral flood damage functions (% of value lost)—see table A1.

over 28% of buildings (panel (A)) and over 23% of total values (panel (B)) are affected by hurricane damage. Additionally, certain populous inland tracts, such as those in Wake County, exhibit similar trends, where over 28% of buildings and 23% of total values suffer non-zero hurricane damage.

Panels (C) and (D) in figure 3 explore the correlation between hurricane impacts on structures and the SVI. Panel (C) reveals that between 25% and 30% of buildings sustain non-zero damage, regardless of their location in coastal or inland regions, across the entire range of SVI scores, showing no significant variation. Panel (D) indicates that the percentage of total value affected by non-zero damages decreases as SVI increases, from a range of 25%–30% down to about 17.5%–22.5% for both coastal and inland areas. This pattern suggests that buildings in lower vulnerability categories, typically situated in zones prone to damage, face higher losses.

Panel (E) in figure 3 focuses on the expected percentage of losses categorized by SVI and occupancy types. It demonstrates that expected losses in inland areas are comparatively minor, under 0.4% across different occupancy classes. Single-family dwellings experience the highest percentage of losses, exceeding 1.2% for the least vulnerable groups, with mobile homes and multi-family buildings facing around 1% and 0.8% losses, respectively, within the residential sector. The industrial sector, particularly within food and drug, heavy, and light industry occupancies, also suffers considerable losses, nearing 1% for groups with low vulnerability. Losses in the commercial

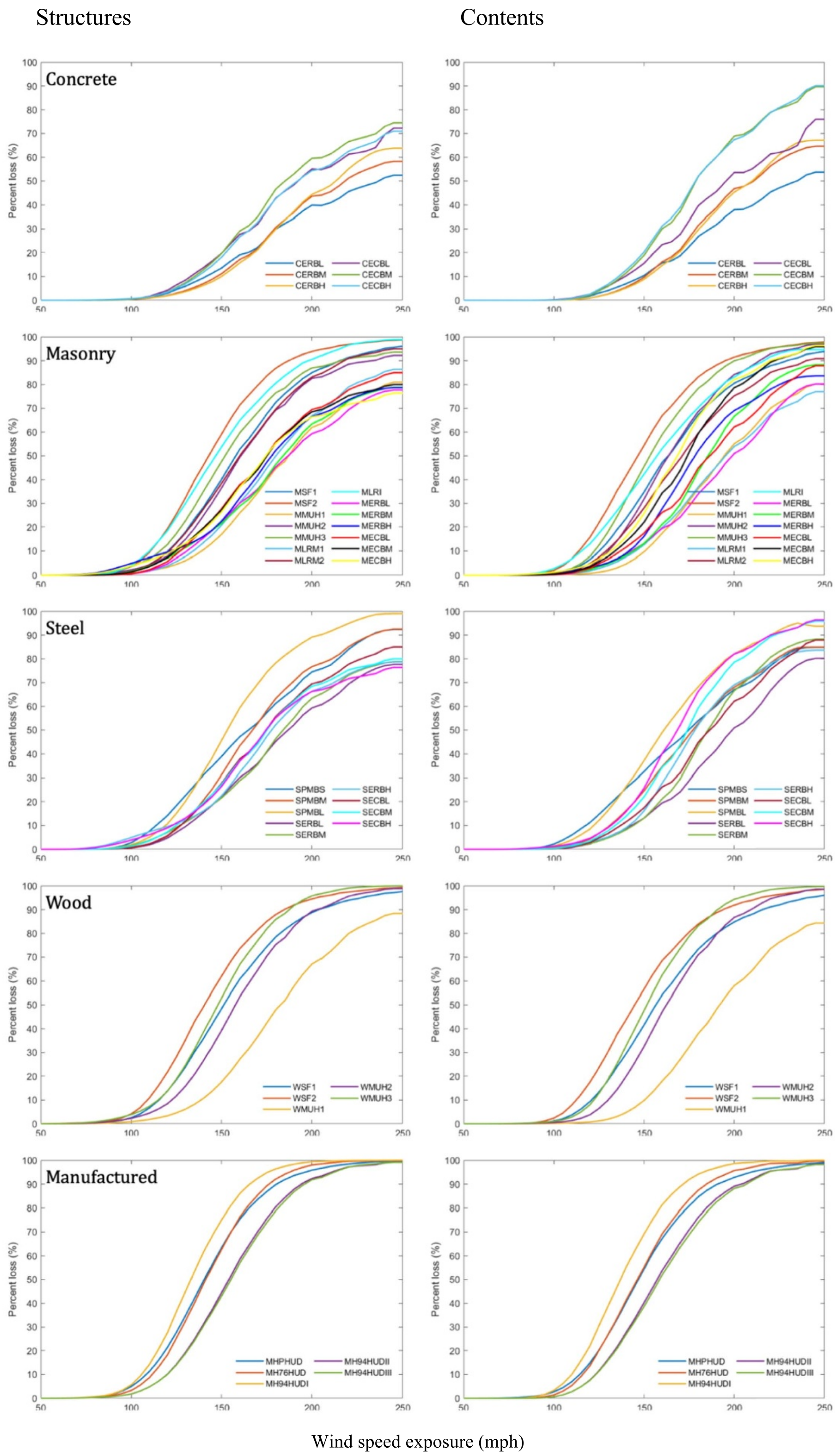

Figure A4. Hazus structural wind damage functions (% of value lost)—see table A1.

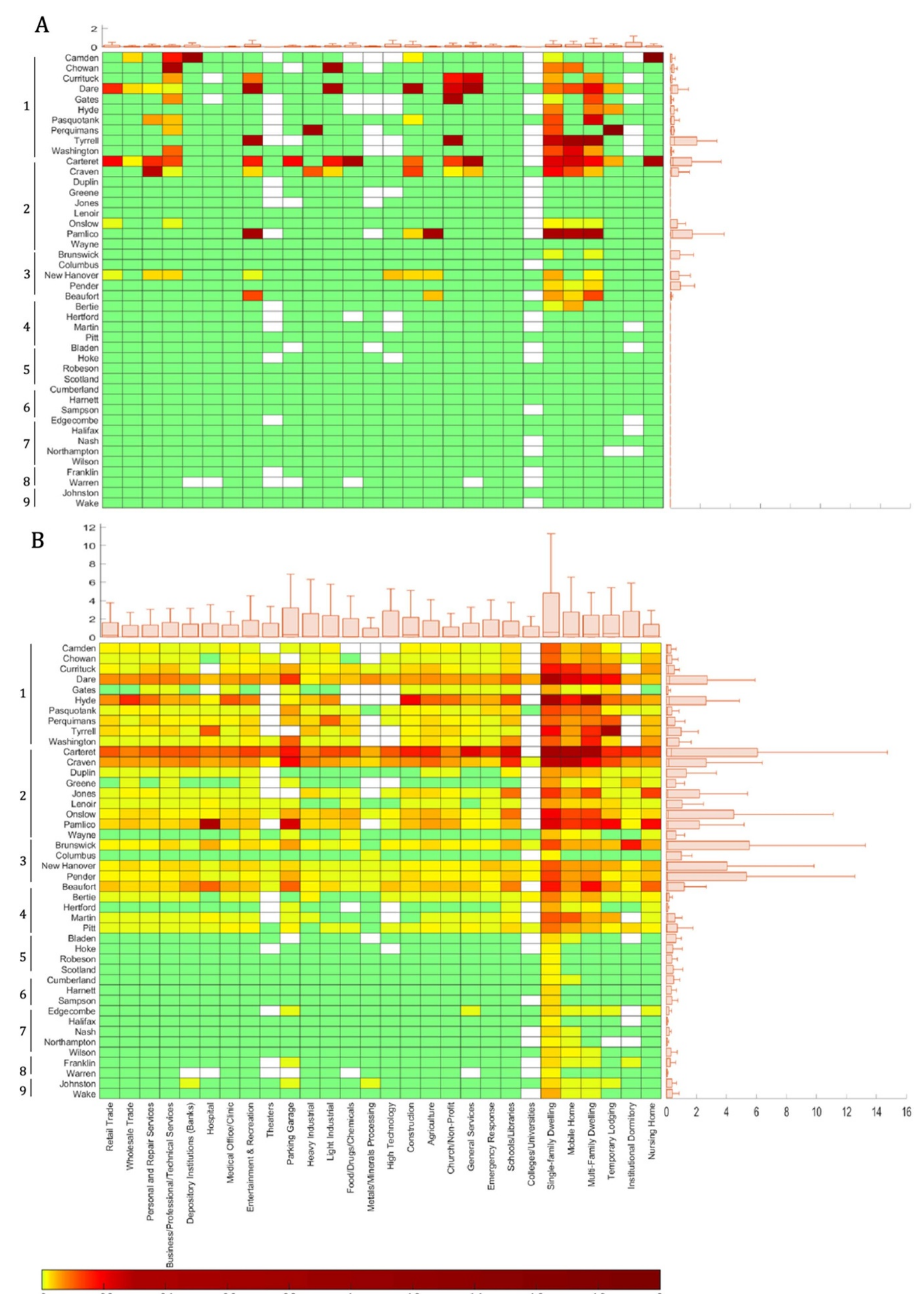

Figure A5. Percent loss of building and content values by county and occupancy class. Regions: (1) Albermarle, (2) Eastern Carolina, (3) Cape Fear, (4) Mid-East, (5) Lumber River, (6) MidCarolina, (7) Upper Coastal Plain, (8) Kerr-Tar, (9) Triangle J.

and public sectors are notably lower, staying below 0.6%.

Figure 4 elucidates the impact of hurricanes on labor, with panels (A) and (B) showing the expected and worst-case scenario labor losses at residence census tracts, respectively. According to panel (A), the highest expected losses are in southeast coastal cities; those are populous areas with high-value houses and facilities and a higher probability of hurricanes. Residents in cities like Wilmington and Morehead are

Table A1. Damage function codes and descriptions.

	Flood		Wind
RES1 1SNB	Single family, 1 story, no basement	WSF1	Wood, Single family, 1 story
RES1 1SWB	Single family, 1 story, basement	WSF2	Wood, Single family, 2+ story
RES1 2SNB	Single family, 2 story, no basement	WMUH1	Wood, Multi-unit, 1 story
RES1 2SWB	Single family, 2 story, basement	WMUH2	Wood, Multi-unit, 2+ story
RES1 3SNB	Single family, 3+ story, no basement	WMUH3	Wood, Multi-unit, 3+ stories
RES1 3SWB	Single family, 3+ story, basement	MSF1	Masonry, Single family, 1 story
RES1 SLNB	Single family, split level, no basement	MSF2	Masonry, Single family, 2+ story
RES1 SLWB	Single family, split level, basement	MMUH1	Masonry, Multi-unit, 1 story
RES2	Mobile home	MMUH2	Masonry, Multi-unit, 2 story
RES3	Apartment	MMUH3	Masonry, Multi-unit, 3+ story
RES4	Hotel/Motel	MLRM1	Masonry, Low-Rise Strip Mall, <15 ft
RES5	Institutional dormitory	MLRM2	Masonry, Low-Rise Strip Mall, >15 ft
RES6	Nursing Home	MLRI	Masonry, Low-rise Industrial/Warehouse/Factory
COM1	Retail	MERBL	Masonry, Engineered Residential, Low-Rise
COM2	Wholesale/Warehouse	MERBM	Masonry, Engineered Residential, Mid-Rise
COM3	Personal/Repair service	MERBH	Masonry, Engineered Residential, High-Rise
COM4	Professional/Technical services	MECBL	Masonry, Engineered Commercial, Low-Rise
COM5	Bank	MECBM	Masonry, Engineered Commercial, Mid-Rise
COM6	Hospital	MECBH	Masonry, Engineered Commercial, High-Rise
COM7	Medical Office/Clinic	CERBL	Concrete, Engineered Residential, Low-Rise
COM8	Entertainment/Recreation	CERBM	Concrete, Engineered Residential, Mid-Rise
COM9	Theatre	CERBH	Concrete, Engineered Residential, High-Rise
COM10	Garage	CECBL	Concrete, Engineered Commercial, Low-Rise
IND1	Heavy Industrial	CECBM	Concrete, Engineered Commercial, Mid-Rise
IND2	Light Industrial	CECBH	Concrete, Engineered Commercial, High-Rise
IND3	Food/Drug/Chemical	SPMBS	Steel, Pre-Engineered Metal, Small
IND4	Metals/Minerals processing	SPMBM	Steel, Pre-Engineered Metal, Medium
IND5	High Technology	SPMBL	Steel, Pre-Engineered Metal, Large
IND6	Construction	SERBL	Steel, Engineered Residential, Low-Rise
ARG1	Agriculture	SERBM	Steel, Engineered Residential, Mid-Rise
REL1	Church	SERBH	Steel, Engineered Residential, High-Rise
GOV1	Government services	SECBL	Steel, Engineered Commercial, Low-Rise
GOV2	Emergency response	SECBM	Steel, Engineered Commercial, Mid-Rise
EDU1	School	SECBH	Steel, Engineered Commercial, High-Rise
EDU2	College/university	MHPFUD	Manufactured Home, Pre-HUD
		MH76HUD	Manufactured Home, 1976 HUD
		MH94HUD-I	Manufactured Home, 1994 HUD Region I
		MH94HUD-II	Manufactured Home, 1994 HUD Region I
		MH94HUD-III	Manufactured Home, 1994 HUD Region III

expected to suffer more than 2% of their real earnings due to hurricanes. The expected losses decrease dramatically as the locations move inland. Since residents with low hurricane risk can commute to the affected places to earn higher wages, we also see that some cities in the northwest of our study area can benefit from hurricanes. The extreme scenarios (panel (B)) reveal that the central and southern areas endure labor losses exceeding 30%, with the zones directly in the hurricane tract facing over 50% losses. In contrast, the northeast coastal regions report labor losses under 10%, attributed to their long distance from the hurricane. There are places realizing positive gains even in the worst scenario; they are far enough away from the hurricane and close enough to the affected areas. Comparing the labor losses with the capital losses in figure 1, the distribution of labor losses no longer follows the distribution of capital losses, which reemphasizes the significance of the redistribution effect of commuting in understanding the socioeconomic consequences of hurricanes.

Panel (C) of figure 4 presents the baseline wages and jobs on the coast and inland. The wage inland shows an obvious decreasing pattern with SVI, while the wages in the coastal area do not. The wages inland are generally higher than those in the coastal area, indicating the existence of wage premiums between coastal and inland areas. The number of jobs in figure 4 shows where most workers live in the studied area. More workers live in the low SVI regions, and more workers live in the inland than in the coastal area. Higher wages and more jobs imply that risk is priced in the labor market; safe inland places attract more workers to live there and generate more job opportunities to support local economic development. Panel (D) in figure 4 demonstrates that the relationship between the measured labor losses decreases with SVI. This pattern is because more high-value

Table A2. Hurricane events affecting North Carolina, simulated tract-level exposure and losses taken from Hazus Loss Library.

Event	Census tracts affected	Exposed value ($ Bn)	Loss ($ Bn)	Loss fraction (%)	Exposure-SVI correlation	Loss-SVI correlation	Loss fraction—SVI correlation
Ana (2015)	86	371	0.006	0.007	−0.227	−0.296	−0.196
Arthur (2014)	69	436	0.054	0.111	−0.212	0.191	0.152
Beryl (2012)	52	504	0.022	0.044	−0.210	−0.328	−0.347
Charley (2004)	241	451	0.307	0.161	−0.205	−0.173	−0.077
Ernesto (2006)	333	380	0.136	0.053	−0.219	−0.410	−0.364
Florence (2018)	613	1795	2.356	0.487	−0.215	−0.385	−0.380
Hanna (2008)	374	661	0.129	0.044	−0.265	−0.331	−0.291
Hermine (2016)	151	745	0.029	0.023	−0.258	−0.343	−0.423
Ian (2022)	1239	1795	0.414	0.039	−0.215	−0.139	−0.037
Irene (2011)	648	780	0.646	0.120	−0.278	−0.116	−0.129
Isabel (2003)	374	632	1.140	0.404	−0.277	−0.081	−0.078
Ivan (2004)	53	1384	0.003	0.008	−0.204	−0.310	−0.225
Matthew (2016)	96	462	0.018	0.023	−0.196	−0.272	−0.274
Michael (2018)	495	1177	0.038	0.009	−0.288	−0.399	−0.296
Ophelia (2005)	195	409	0.410	0.273	−0.195	−0.398	−0.401

capital stays in the lower SVI regions, and capital losses dominate the changes in labor earnings after hurricanes. This effect is more phenomenal in the coastal areas than inland areas.

ORCID iDs

Dahui Liu https://orcid.org/0009-0008-2157-3314
Junkan Li https://orcid.org/0000-0003-1766-2636
Ian Sue Wing https://orcid.org/0000-0003-1177-3589

References

Apivatanagul P, Davidson R, Blanton B and Nozick L 2011 Long-term regional hurricane hazard analysis for wind and storm surge *Coast. Eng.* **58** 499–509

Atkinson J *et al* 2008 Hurricane storm surge and wave modeling in southern Louisiana: a brief overview *Estuarine and Coastal Modeling X* ed M Spaulding (ASCE) pp 467–506

Bakkensen L, Shi X and Zurita B 2018 The impact of disaster data on estimating damage determinants and climate costs *Econ. Disasters Clim. Change* **2** 49–71

Belasen A R and Polachek S W 2008 How hurricanes affect wages and employment in local labor markets *Am. Econ. Rev.* **98** 49–53

Bellemare M F and Wichman C J 2020 Elasticities and the inverse hyperbolic sine transformation *Oxf. Bull Econ. Stat.* **82** 50–61

Benevolenza M A and DeRigne L 2019 The impact of climate change and natural disasters on vulnerable populations: a systematic review of literature *J. Hum. Behav. Soc. Environ.* **29** 266–81

Bernstein A, Gustafson M and Lewis R 2021 Disaster on the horizon: the price effect of sea level rise *J. Financ. Econ.* **134** 253–72

Blanton B, Dresback K, Colle B, Kolar R, Vergara H, Hong Y, Leonardo N, Davidson R, Nozick L and Wachtendorf T 2018 An integrated scenario ensemble-based framework for hurricane evacuation modeling: part 2—Hazard modeling *Risk Anal.* **40** 117–33

Blanton B, Luettich R, Vickery P, Hanson J, Slover K and Langan T 2012 North Carolina Floodplain mapping program: coastal flood insurance study—production simulations and statistical analyses *Technical Report TR-12-03* (Renaissance Computing Institute, The University of North Carolina at Chapel Hill)

Blanton B, Seim H, Luettich R, Lynch D, Werner F, Smith K, Voulgaris G, Bingham F and Way F 2004 Barotropic tides in the South Atlantic Bight *J. Geophys. Res.* **109** C12024

Bloemendaal N, Haigh I, de Moel H, Muis S, Haarsma R and Aerts J 2020 Generation of a global synthetic tropical cyclone hazard dataset using STORM *Sci. Data* **7** 40

Brackins J and Kalyanapu A 2020 Evaluation of parametric precipitation models in reproducing tropical cyclone rainfall patterns *J. Hydrol.* **580** 124255

Burton C G 2010 Social vulnerability and hurricane impact modeling *Nat. Hazards Rev.* **11** 58–68

Centers for Disease Control and Prevention/Agency for Toxic Substances and Disease Registry (CDC/ATSDR) 2020 CDC SVI documentation 2020 (available at: www.atsdr.cdc.gov/placeandhealth/svi/documentation/SVI_documentation_2020.html)

Chavas D R and Lin N 2016 A model for the complete radial structure of the tropical cyclone wind field. Part II: wind field variability *J. Atmos. Sci.* **73** 3093–113

Chavas D R, Lin N and Emanuel K 2015 A model for the complete radial structure of the tropical cyclone wind field. Part I: comparison with observed structure *J. Atmos. Sci.* **72** 3647–62

Cutter S L, Boruff B J and Shirley W L 2003 Social vulnerability to environmental hazards *Soc. Sci. Q.* **84** 242–61

Davidson R *et al* 2018 An integrated scenario ensemble-based framework for hurricane evacuation modeling: part 1—Evacuation modeling *Risk Anal.* **40** 97–116

Dietrich J, Zijlema M, Westerink J, Holthuijsen L, Dawson C, L. R Jr, Jensen R, Smith J, Stelling G and Stone G 2010 Modeling hurricane waves and storm surge using integrally-coupled, scalable computations *Coast. Eng.* **58** 45–65

Done J, Simmons K and Czajkowski J 2018 Relationship between residential losses and hurricane winds: role of the Florida building code *ASCE-ASME J. Risk Uncertain. Eng. Syst.* A **4** 04018001

Dresback K *et al* 2013 Skill assessment of a real-time forecast system utilizing a coupled hydrologic and coastal hydrodynamic model during Hurricane Irene (2011) *Cont. Shelf Res.* **71** 78–94

ESP Associates Inc 2021 Southeastern North Carolina regional hazard mitigation plan (Onslow County Government) (available at: www.onslowcountync.gov/DocumentCenter/

View/16736/00–2021-SENC-RHMP-FINAL-Full-Document?bidId=)
Federal Emergency Management Agency 2022a Hazus hurricane model technical manual 5.1 (available at: www.fema.gov/sites/default/files/documents/fema_hazus-hurricane-model-technical-manual-5-1.pdf)
Federal Emergency Management Agency 2022b Hazus flood model technical manual 5.1 (available at: www.fema.gov/sites/default/files/documents/fema_hazus-flood-model-technical-manual-5-1.pdf)
Federal Emergency Management Agency 2022c Hazus inventory technical manual 6.0 (available at: www.fema.gov/sites/default/files/documents/fema_hazus-inventory-technical-manual-6.pdf)
Federal Emergency Management Agency 2023 Hazus loss library (available at: https://hazards.fema.gov/hll/library) (Accessed 5 December 2023)
Flanagan B, Hallisey A, Adams E and Lavery A 2018 Measuring community vulnerability to natural and anthropogenic hazards: the centers for disease control and prevention's social vulnerability index *J. Environ. Health* **80** 34–36
Geiger T, Frieler K and Levermann A 2016 High-income does not protect against hurricane losses *Environ. Res. Lett.* **11** 084012
Gesch D, Oimoen M, Greenlee S, Nelson C, Steuck M and Tyler D 2002 The national elevation dataset *Photogramm. Eng. Remote Sens.* **68** 5–32
Gori A, Lin N and Xi D 2020 Tropical cyclone compound flood hazard assessment: from investigating drivers to quantifying extreme water levels *Earth's Future* **8** e2020EF001660
Gourevitch J, Kousky C, Liao Y, Nolte C, Pollack A, Porter J and Weill J 2023 Unpriced climate risk and the potential consequences of overvaluation in US housing markets *Nat. Clim. Change* **13** 250–7
Groen J, Kutzbach M and Polivka A 2020 Storms and jobs: the effect of hurricanes on individuals' employment and earnings over the long term *J. Labor Econ.* **38** 653–85
Hanson J L, Forte M F, Blanton B, Gravens M and Vickery P 2013 Coastal storm surge analysis: storm surge results. report 5: intermediate submission no. 3 *Technical Report* (DTIC Document)
Hendricks E, Knievel J and Nolan D 2021 Evaluation of boundary layer and urban canopy parameterizations for simulating wind in miami during Hurricane Irma (2017) *Mon. Weather Rev.* **149** 2321–49
Holland G J 1980 An analytic model of the wind and pressure profiles in hurricanes
Homer C G, Fry J A and Barnes C A 2012 *The National Land Cover Database (No. 2012–3020)* (US Geological Survey)
Iglesias V *et al* 2021 Risky development: increasing exposure to natural hazards in the United States *Earth's Future* **9** e2020EF001795
IMPLAN® model 2019 Data, using inputs provided by the user and IMPLAN group LLC, IMPLAN system (data and software), 16905 Northcross Dr, Suite 120, Huntersville, NC 28078 (available at: www.IMPLAN.com)
Klima K, Lin N, Emanuel K, Morgan M G and Grossmann I 2012 Hurricane modification and adaptation in Miami-Dade County, Florida *Environ. Sci. Technol.* **46** 636–42
Landsea C and Franklin J 2013 Atlantic hurricane database uncertainty and presentation of a new database format *Mon. Weather Rev.* **141** 3576–92
Liu Q, Wu L and Qin N 2022 Wind gusts associated with tornado-scale vortices in the tropical cyclone boundary layer: a numerical simulation *Front. Earth Sci.* **10** 945058
Liu Q, Wu L, Qin N and Li Y 2021 Storm-scale and fine-scale boundary layer structures of tropical cyclones simulated with the WRF-LES framework *JGR Atmos.* **126** e2021JD035511
Luettich R A and Westerink J J 1992 A three dimensional circulation model using a direct stress solution over the vertical *Computational Methods in Water Resources IX, Volume 2: Mathematical Modeling in Water Resources* ed T Russell (Computational Mechanics Publications)
Mazumder R, Enderami S and Sutley E 2023 A novel framework to study community-level social and physical impacts of hurricane-induced winds through synthetic scenario analysis *Front. Built Environ.* **9** 1005264
Metzler R, Ellen I and Li X 2021 Localized commercial effects from natural disasters: the case of Hurricane Sandy and New York City *Reg. Sci. Urban Econ.* **86** 103608
Nair S, King A, Gulledge J, Preston B, McManamay R and Clark C 2020 Economic losses from extreme weather in the U.S. Gulf Coast region: spatially differential contributions of climate hazard and socioeconomic exposure and vulnerability *Environ. Res. Lett.* **15** 074038
Nakamura J, Lall U, Kushnir Y and Harr P A 2024 A saturated stochastic simulator: synthetic US Gulf coast tropical cyclone precipitation fields *Nat. Hazards* **120** 1295–318
Niedoroda A, Resio D, Toro G, Divoky D, Das H and Reed C 2010 Analysis of the coastal Mississippi storm surge hazard *Ocean Eng.* **37** 82–90
NOAA National Centers for Environmental Information 2023 Monthly global climate report 2023 for December 2022 (available at: https://www.ncei.noaa.gov/access/monitoring/monthlyreport/global/202300) (Accessed 14 August 2024)
Nofal O, van de Lindt J, Do T, Yan G, Hamideh S, Cox D and Dietrich J 2021 Methodology for regional multihazard hurricane damage and risk assessment *J. Struct. Eng.* **147** 04021185
Nolan D, McNoldy B and Yunge J 2021a Evaluation of the surface wind field over land in WRF simulations of Hurricane Wilma (2005). Part I: model initialization and simulation validation *Mon. Weather Rev.* **149** 679–95
Nolan D, McNoldy B, Yunge J, Masters F J and Giammanco I M 2021b Evaluation of the surface wind field over land in WRF simulations of Hurricane Wilma (2005). Part II: surface winds, inflow angles, and boundary layer profiles *Mon. Weather Rev.* **149** 697–713
Ortega F and Taspinar S 2018 Rising sea levels and sinking property values: hurricane Sandy and New York's housing market *J. Urban Econ.* **106** 81–100
Pielke R 2021 Economic 'normalisation' of disaster losses 1998–2020: a literature review and assessment *Environ. Hazards* **20** 93–111
Pollack A B, Sue Wing I and Nolte C 2022 Aggregation bias and its drivers in large-scale flood loss estimation: a Massachusetts case study *J. Flood Risk Manage.* **15** e12851
Pollack A B, Wrenn D H, Nolte C and Wing I S 2023 Potential benefits in remapping the special flood hazard area: evidence from the US housing market *J. Housing Econ.* **61** 101956
Rotunno R, Chen Y, Wang W, Davis C, Dudhia J and Holland G J 2009 Large-eddy simulation of an idealized tropical cyclone *Bull. Am. Meteorol. Soc.* **90** 1783–8
Ruggles S, Flood S, Sobek M, Backman D, Chen A, Cooper G, Richards S, Rogers R and Schouweiler M 2024 *IPUMS USA: Version 15.0* (IPUMS) (https://doi.org/10.18128/D010.V15.0)
Rybski D, Prahl B and Kropp J 2017 Comment on 'High-income does not protect against hurricane losses *Environ. Res. Lett.* **12** 098001
Sanchez Gomez M, Lundquist J, Deskos G, Arwade S R, Myers A T and Hajjar J F 2023 Wind fields in Category 1–3 tropical cyclones are not fully represented in wind turbine design standards *JGR Atmos.* **128** e2023JD039233
Shao W, Jackson N, Ha H and Winemiller T 2020 Assessing community vulnerability to floods and hurricanes along the Gulf Coast of the United States *Disasters* **44** 518–47
Smith A and Katz R 2013 US billion-dollar weather and climate disasters; data sources, trends, accuracy and biases *Nat. Hazards* **67** 387–410
Smith A and Matthews J 2015 Quantifying uncertainty and variable sensitivity within the US billion-dollar weather and climate disaster cost estimates *Nat. Hazards* **77** 1829–51

Stern D, Brya G, Lee C and Doyle J D 2021 Estimating the risk of extreme wind gusts in tropical cyclones using idealized large-eddy simulations and a statistical-dynamical model *Mon. Weather Rev.* **149** 4183–204

Sue Wing I, Rose A, Wei D and Wein A 2023 The long shadow of a major disaster: modeled dynamic impacts of the hypothetical HayWired earthquake on California's economy *Int. Reg. Sci. Rev.* accepted (https://doi.org/10.1177/01600176231202451)

Tate E, Rahman M, Emrich C and Sampson C 2021 Flood exposure and social vulnerability in the United States *Nat. Hazards* **106** 435–57

Toro G, Resio D, Divoky D, Niedoroda A and Reed C 2010 Efficient joint-probability methods for hurricane surge frequency analysis *Ocean Eng.* **37** 125–34

US Army Corps of Engineers 2022 National structure inventory: technical documentation (available at: www.hec.usace.army.mil/confluence/nsi/technicalreferences/latest/technical-documentation)

US Census Bureau 2023 LEHD origin-destination employment statistics (LODES) dataset structure: format version 8.0 (Census Bureau) (available at: https://lehd.ces.census.gov/data/lodes/LODES8/LODESTechDoc8.0.pdf)

Vickery P and Blanton B 2008 North Carolina coastal flood analysis system: hurricane parameter development *Technical Report TR-08-06* (Renaissance Computing Institute, University of North Carolina at Chapel Hill)

Vickery P, Skerlj P, Lin J, Twisdale L, Young M and Lavelle F 2006 HAZUS-MH Hurricane model methodology II: damage and loss estimation *Nat. Hazards Rev.* **7** 94–103

Vickery P, Skerlj P and Twisdale L 2000 Simulation of hurricane risk in the U.S. using an empirical track model *J. Struct. Eng.* **126** 1222–37

Vosper E, Watson P, Harris L, McRae A, Santos-Rodriguez R, Aitchison L and Mitchell D 2023 Deep learning for downscaling tropical cyclone rainfall to hazard-relevant spatial scales *J. Geophys. Res. Atmos.* **128** e2022JD038163

Wahl T, Jain S, Bender J, Meyers S D and Luther M 2015 Increasing risk of compound flooding from storm surge and rainfall for major US cities *Nat. Clim. Change* **5** 1093–7

Wang S, Lin N and Gori A 2022 Investigation of tropical cyclone wind models with application to storm tide simulations *JGR Atmos.* **127** 2021JDo36359

Westerink J J, Luettich R, Feyen J, Atkinson J, Dawson C, Roberts H, Powell M, Dunion J, Kubatko E and Pourtaheri H 2008 A basin- to channel-scale unstructured grid hurricane storm surge model applied to Southern Louisiana *Mon. Weather Rev.* **136** 833–64

Wu L, Liu Q and Li Y 2018 Prevalence of tornado-scale vortices in the tropical cyclone eyewall *Proc. Natl Acad. Sci.* **115** 8307–10

Wu X, Xu Z, Liu H, Guo J and Zhou L 2019 What are the impacts of tropical cyclones on employment? An analysis based on meta-regression, weather *Clim. Soc.* **11** 259–75

Wurman J and Kosiba K 2018 The role of small-scale vortices in enhancing surface winds and damage in hurricane harvey (2017) *Mon. Weather Rev.* **146** 713–22

Yang J, Duan Z, Chen Y and Ou J 2023 Assessing parametric rainfall models in reproducing tropical cyclone rainfall characteristics *Atmos. Res.* **288** 106726

Zhai A and Jiang J 2014 Dependence of US hurricane economic loss on maximum wind speed and storm size *Environ. Res. Lett.* **9** 064019

Zhang Y *et al* 2020 Simulating compound flooding events in a hurricane *Ocean Dyn.* **70** 621–40